

國立臺灣大學工學院機械工程學研究所

碩士論文

Department of Mechanical Engineering

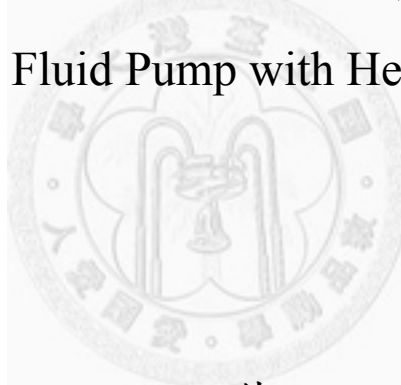
College of Engineering

National Taiwan University

Master Thesis

一種新型螺旋爪式轉子流體幫浦之設計

Design of a New Fluid Pump with Helical Claw Rotors



王心偉

Hsin-Wei Wang

指導教授：鍾添東 博士

Advisor: Tien-Tung Chung, Ph.D.

中華民國 99 年 7 月

July, 2010



# 國立臺灣大學碩博士學位論文

## 口試委員會審定書

一種新型螺旋爪式轉子流體幫浦之設計

Design of a New Fluid Pump with Helical Claw Rotors

本論文係王心偉君（R97522632）在國立臺灣大學機械工程學系完成之碩士學位論文，於民國 99 年 07 月 27 日承下列考試委員審查通過及口試及格，特此證明

口試委員：（指導教授）

鍾添東

劉 霆

林恆毅

鍾添東

劉 霆

林恆毅

系主任

張所鎡

張所鎡

（簽名）

## 誌謝

研究所求學時光轉瞬即逝，省視自己兩年的收穫，除了學業上的成就，在團隊合作、待人接物上都比以往更加圓融成熟。這本碩士論文的完成，要感謝許多人的指導及幫忙，首先要感謝的是指導教授鍾添東老師，在轉子外型繪製及 AutoLISP 程式撰寫上給我許多啟發，在老師的指導下也讓我更注重細節。再來要感謝良峰塑膠機械股份有限公司的許蒼林先生及工程師林恆毅博士，在轉子外型設計上給予我建議與指導；口試委員劉霆老師在轉子曲面設計上提供許多未曾思考過的想法，讓這份論文更加完整。實驗室學長林錦德，同學朱志祥、李哲維、龔玲玉平時的切磋砥礪及日常生活上諸多協助，讓我能夠在愉悅的心情下完成論文，遇到問題也能夠互相討論，良好的同窗氣氛是這兩年研究生活中我最珍惜的回憶。另外，好朋友們並沒有因為我每天躲在實驗室而失聯，MSN 上的打氣或是相約吃飯的閒聊都讓身心能夠從緊湊的研究壓力中舒緩，充飽電更有衝勁。

最後，要感謝我的家人，我親愛的父母親，一直以來無條件的支持著我，為我付出一切，沒有你們就沒有今天的我；親愛的奶奶跟外公外婆，時時關心著我、為我的一切感到開心；還有在天上的爺爺，孫子已經拿到碩士學位了，希望我的表現能夠讓您感到驕傲。僅以這本碩士論文，獻給你們。



## 中文摘要

本論文提出新式螺旋爪式轉子之設計，該設計可應用於流體幫浦。該螺旋爪式轉子設計包含截面輪廓及軸向旋轉。首先，定義爪式轉子之輪廓曲線為其截面，並建立其參數化模型，是以該設計爪式轉子輪廓曲線上之任一點均可由輸入指定參數獲得，且轉子輪廓外形可由設計變數調整。將爪式轉子應用於流體幫浦，其幫浦效率及流量也可藉由此參數化模型求得，意即使用者可依其需求幫浦性能設定轉子之設計變數。考量爪式轉子幫浦在運作過程中產生的周期性振動容易產生噪音及造成機構損壞，將螺旋設計應用於爪式轉子，藉由對軸向各截面進行連續相位移，達到疊合不連續流量的作用，可穩定排放以降低振動。螺旋爪式轉子幫浦之排放為單向，容易造成額外應力作用於幫浦機構，是以本研究提出一改良式螺旋爪式轉子，其弧形之側邊構造可達雙向排放之功效。為能準確評估爪式轉子幫浦及螺旋爪式轉子幫浦運轉時每一瞬間之流量，本研究撰寫一電腦運算程式，對各不同設計之爪式轉子幫浦進行分析，分析結果顯示螺旋爪式轉子幫浦的確可有效穩定排放流量，達降低振動之功效，提升幫浦效率。

關鍵字：迴轉式幫浦、爪式轉子、螺旋轉子、參數化模型

## **Abstract**

This thesis describes the study of an innovative helical claw rotor design for fluid pump. Firstly, the contour of the claw rotor pair is constructed and is set into parametric model, and the design variables which can lead to the required performance, such as flow rate, is determined by the parametric model. By the computer aided design program, the claw rotor model is obtained after inputting values of the design variables. Due to the pulsation problem caused by the discontinuous pumping flow, the helical design is applied to the rotor pair. Helical design can be considered as phase shifting an indefinite number of the cross-sections of the claw rotor pair and superimposing the discharge flow. Therefore, the discharge flow would become more continuous and the pulsation would be decreased. Taken the stress and bending torque caused by the unidirectional discharging flow of the helical claw rotor pump into consideration, the rotor pair which could make a two-way discharging process would be an ideal design. Then a curve-sided type helical claw rotor pair, which is the modification of the helical claw rotor pair, is designed. Next, a calculation program is proposed in order to analyze the performances of these claw rotor pump designs, and the conventional claw rotor pump can therefore be compared with the two helical designs. The analysis shows that the

pumping flows of the helical claw rotor pump and the curve-sided type helical claw rotor pump are more continuous than the conventional design, which results in less flow pulsations and higher efficiencies. In conclusion, the helical designs of claw rotor fluid pump are worthy to develop.

*Keywords: Rotary pump, claw rotor, helical rotor, parametric modeling program.*



# Table of Content

論文口試委員會審定書 .....	I
誌謝 .....	II
中文摘要 .....	III
Abstract.....	IV
Table of Content .....	VI
List of Figures.....	IX
List of Tables .....	XIII
Chapter 1 Introduction .....	1
1.1 Introduction .....	1
1.2 Comparison of rotary pumps .....	4
1.3 Literature and patent review .....	9
1.4 Research objective.....	17
Chapter 2 Mechanical principles and pump theories .....	18
2.1 Specific flow rate and area efficiency .....	18
2.2 Leakage theory .....	20
2.3 Pump efficiency.....	21

Chapter 3	Modified designs of the claw rotor pump.....	23
3.1	Fundamental of the claw rotor pump.....	23
3.2	Modified designs of the claw rotor.....	30
Chapter 4	Performance analysis of the claw rotor pump .....	39
4.1	Volumetric flow rate calculation.....	39
4.2	Flow rate analysis of the claw rotor pump .....	43
4.3	Flow rate analysis of the helical claw rotor pump.....	46
4.4	Flow rate analysis of the curve-sided type helical claw rotor pump .....	51
4.5	Comparison of the helical designed claw rotor pumps .....	61
Chapter 5	Conclusions and suggestions.....	64
5.1	Conclusions .....	64
5.2	Suggestions.....	66
References	.....	68
Appendix A	AutoLISP program for flow rate calculation.....	71
Appendix B	Flow rate data of claw rotor pump .....	78
Appendix C	Flow rate data of curve-sided type helical claw rotor pumps .....	85
C.1	Flow rate data of the arc shape type .....	85
C.2	Flow rate data of the parabolic type.....	92

C.3 Flow rate data of the yoke shape type.....	99
Vitae.....	106



## List of Figures

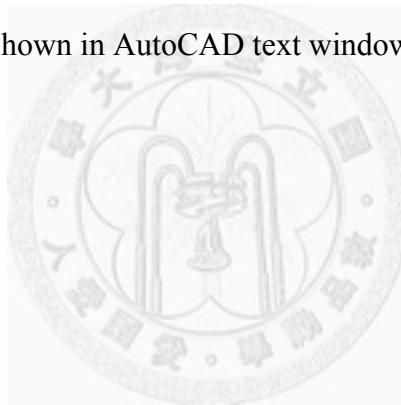
Figure 1-1 Classification of pumps .....	1
Figure 1-2 External gear pump .....	5
Figure 1-3 Internal gear pump .....	5
Figure 1-4 Lobe pump .....	7
Figure 1-5 Screw pump .....	8
Figure 1-6 Operation process of a screw pump .....	8
Figure 1-7 Single claw rotor pump .....	10
Figure 1-8 Double claw rotor .....	10
Figure 1-9 Vacuum processes of claw rotor pump .....	10
Figure 1-10 Single claw rotor design by involute method .....	11
Figure 1-11 Double claw rotor design by involute method .....	11
Figure 1-12 Design region of the parameter of 1-claw rotor .....	12
Figure 1-13 1-claw rotor drawn by cycloid method .....	12
Figure 1-14 3-Claw rotor .....	13
Figure 1-15 Smooth shape 2-claw rotor .....	13
Figure 1-16 Identical symmetrically-shaped 2-claw rotor .....	14

Figure 1-17 Comparison of specific flow rate in designate pitch ratios.....	15
Figure 1-18 Pulsation as the result of flow fluctuation .....	16
Figure 1-19 Helically toothed lobes .....	16
Figure 2-1 Carry over volume of the claw rotor pair .....	19
Figure 2-2 Schematic of clearance flow .....	20
Figure 3-1 Parameters of the driving rotor .....	23
Figure 3-2 Generating process of curve F .....	26
Figure 3-3 Generating process of the right rotor .....	27
Figure 3-4 Distance function of angular coordinate $\theta$ .....	27
Figure 3-5 Parameters for the generation of the conjugate rotor.....	29
Figure 3-6 Rotation angle is linear to the axial direction .....	31
Figure 3-7 Solid model of the helical claw rotor pair.....	32
Figure 3-8 Helical claw rotors in the housing chamber.....	32
Figure 3-9 System momentum of the claw rotor pump.....	33
Figure 3-10 Curve formed by rolling up a plane with an arc on it to a cylinder .....	35
Figure 3-11 Solid model of the curve-sided type helical claw rotor pair .....	35
Figure 3-12 Curve shapes on a plane .....	36
Figure 3-13 Two curve-sided type helical claw rotor pairs .....	37



Figure 3-14 Discharge process of the curve-sided helical claw rotor pump .....	38
Figure 4-1 Fluid volume is the subtraction between chamber volume and rotor volume .....	41
Figure 4-2 Area integration of the right rotor .....	41
Figure 4-3 Derivation for the fluid volume of the helical claw rotor pump .....	42
Figure 4-5 Flow rate in 1 period of a 6-claw rotor pump .....	44
Figure 4-6 Flow rate of pumps with different claw numbers .....	45
Figure 4-7 Flow rate of the 4-claw helical rotor pump .....	48
Figure 4-8 Flow rate of the 5-claw helical rotor pump .....	49
Figure 4-9 Flow rate of the 6-claw helical rotor pump .....	50
Figure 4-10 Flow rate of 4-claw arc shape curve-sided type pump .....	52
Figure 4-11 Flow rate of 5-claw arc shape curve-sided type pump .....	53
Figure 4-12 Flow rate of 6-claw arc shape curve-sided type pump .....	53
Figure 4-13 Comparison of flow rate between helical and arc shape curve-sided claw rotor pump .....	55
Figure 4-14 Flow rate of 4-claw parabolic curve-sided type pump .....	56
Figure 4-15 Flow rate of 5-claw parabolic curve-sided type pump .....	56
Figure 4-16 Flow rate of 6-claw parabolic curve-sided type pump .....	57

Figure 4-17 Flow rate of 4-claw yoke shape curve-sided type pump .....	58
Figure 4-18 Flow rate of 5-claw yoke shape curve-sided type pump .....	59
Figure 4-19 Flow rate of 6-claw yoke shape curve-sided type pump .....	59
Figure 4-20 Flow rate of different helical types of 4-claw rotor pumps .....	62
Figure A-1 AutoCAD Text Window .....	71
Figure A-2 Loading the calculation program .....	75
Figure A-3 Flow rate calculation commands (FLOW) .....	76
Figure A-4 Analysis result shown in AutoCAD text window.....	77



## List of Tables

Table 1-1 Comparison of common rotary pumps .....	9
Table 4-1 Design variables of claw rotor pumps .....	45
Table 4-2 Fluctuation coefficient of different number of claws .....	46
Table 4-3 Fluctuation coefficients of the 4-claw helical rotor pump.....	48
Table 4-4 Fluctuation coefficients of the 5-claw helical rotor pump.....	49
Table 4-5 Fluctuation coefficients of the 6-claw helical rotor pump.....	50
Table 4-6 Fluctuation coefficients of arc shape curve-sided type pumps.....	54
Table 4-7 Fluctuation coefficients of parabolic curve-sided type pumps.....	57
Table 4-8 Fluctuation coefficients of yoke shape curve-sided type pumps.....	60
Table 4-9 Fluctuation coefficients of different helical types of claw rotor pumps.....	62
Table A-1 AutoLISP commands to analyze different type of claw rotor pump .....	76
Table B-1 Data of 4-claw helical claw rotor pump .....	78
Table B-2 Data of 5-claw helical claw rotor pump .....	81
Table B-3 Data of 6-claw helical claw rotor pump .....	83
Table C-2 Data of 5-claw arc shape curve-sided type helical claw rotor pump.....	88
Table C-3 Data of 6-claw arc shape curve-sided type helical claw rotor pump.....	90

Table C-5 Data of 5-claw parabolic curve-sided type helical claw rotor pump .....	95
Table C-6 Data of 6-claw parabolic curve-sided type helical claw rotor pump .....	97
Table C-8 Data of 5-claw yoke shape curve-sided type helical claw rotor pump .....	102
Table C-9 Data of 6-claw yoke shape curve-sided type helical claw rotor pump .....	104



# Chapter 1 Introduction

## 1.1 Introduction

Mechanical fluid pumps are widely used in the modern industry, agriculture industry and household living because of the simple and reliable structure. They are applied to pump oil, irrigate crops, extract groundwater and supply household water.

According to their operation processes and structures, liquid pumps are classified into two categories: positive displacement pump and non-positive displacement pump, also named dynamic pump, as shown in Fig. 1-1. These two kinds of pump are both widely used in hydraulic systems.

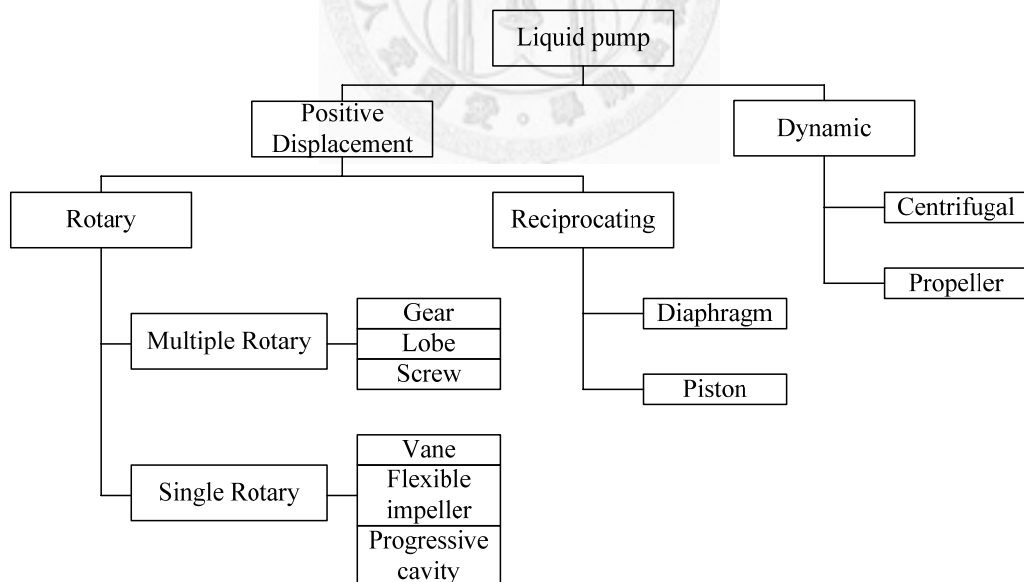


Figure 1-1 Classification of pumps [1]

A positive displacement pump causes a fluid to move by trapping a fixed amount of it then forcing that trapped volume into the discharge pipe. A positive displacement pump can be further classified according to the mechanism used to move the fluid:

#### 1. Rotary type

It includes the gear, lobe, screw, shuttle block, flexible vane or sliding vane, helical twisted roots or liquid ring vacuum pumps. By using the principles of rotation, positive displacement rotary pumps can move fluid. The rotation of the pump creates the vacuum area which captures and draws in the liquid, and the operation process of rotary pump is very efficient. However, positive displacement rotary pumps also have their weaknesses. Because of the nature of the pump, the clearance between the rotating pump and the outer edge must be very close, requiring that the pumps rotate at a slow, steady speed. If rotary pumps are operated at high speeds, the fluids will cause erosion. Rotary pumps that experience such erosion eventually show signs of enlarged clearances, which allow liquid to slip through and detract from the efficiency of the pump.

#### 2. Reciprocating type

It includes diaphragm and piston pumps. Reciprocating type pump has an expanding cavity on the suction side and a decreasing cavity on the discharge side.

While the suction side expands the liquid would flow into the pumps and then flows out of the discharge as the cavity collapses. The volume is constant given each cycle of operation.

Dynamic pumps, including centrifugal and propeller pumps, are those in which kinetic energy is added to the fluid by increasing the flow velocity. This increase in energy is converted to a gain in potential energy (pressure) when the velocity is reduced prior to or as the flow exits the pump into the discharge pipe. This conversion of kinetic energy to pressure can be explained by the first law of thermodynamics or more specifically by Bernoulli's principle. Dynamic pumps can be further subdivided according to the means in which the velocity gain is achieved.

These types of pumps have a number of characteristics: continuous energy, conversion of added energy to increase in kinetic energy, conversion of increased velocity (kinetic energy) to an increase in pressure head.

One practical difference between dynamic and positive displacement pumps is their ability to operate under closed valve conditions. Positive displacement pumps physically displace the fluid; hence closing a valve downstream of a positive displacement pump will result in a continual build up in pressure resulting in

mechanical failure of either pipeline or pump. Dynamic pumps differ in that they can be safely operated under closed valve conditions (for short periods of time).

## **1.2 Comparison of rotary pumps**

Compared with dynamic pumps, positive displacement rotary pumps have closed chambers, hence have higher volumetric efficiency. The three major kinds of rotary positive displacement pumps will be introduced as the followings:

### **1. Gear pump**

Gear pumps use the meshing of gears to pump fluid by displacement. They are one of the most common types of pumps for hydraulic fluid power applications. Gear pumps however are also widely used in chemical installations to pump fluid with a certain viscosity. There are two main variations: external gear pumps which use two external spur gears, as shown in Fig. 1-2, and internal gear pumps which use an external and an internal spur gear, as shown in Fig. 1-3. Gear pumps are fixed displacement, meaning they pump a constant amount of fluid for each revolution. As the gears rotate they separate on the intake side of the pump, creating a void and suction which is filled by fluid. The fluid is carried by the gears to the discharge side of the pump, where the meshing of the gears displaces the fluid. The mechanical clearances are small—on the



order of a thousandth of an inch (micrometers). The tight clearances, along with the speed of rotation, effectively prevent the fluid from leaking backwards. According to researches, under constant pressure rotation, the amount of leakages of a gear pump between two gears, gears and chamber maintains constant. That means the volumetric efficiency will be higher when the rotation speed increases.

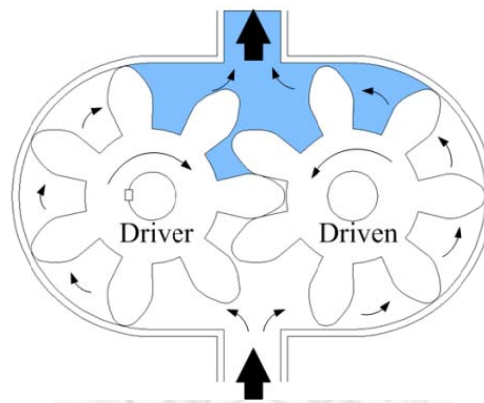


Figure 1-2 External gear pump [2]

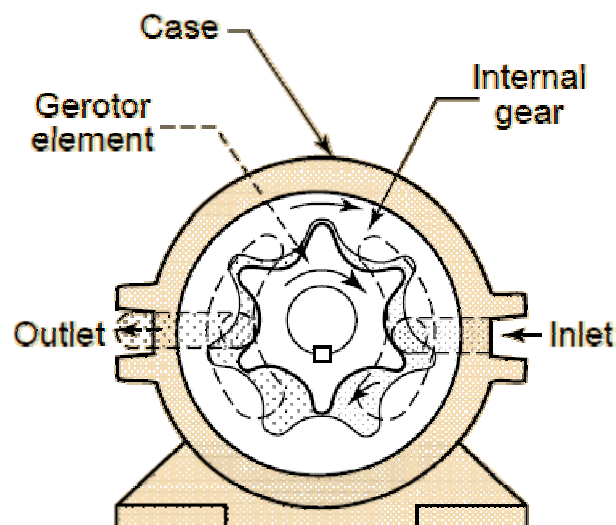


Figure 1-3 Internal gear pump [2]

## 2. Lobe pump

Lobe pumps are similar to external gear pumps in operation in that fluid flows around the interior of the casing, as shown in Fig. 1-4. Unlike external gear pumps, however, the lobes do not make contact. Lobe contact is prevented by external timing gears located in the gearbox. As the lobes come out of mesh, they create expanding volume on the inlet side of the pump. Liquid flows into the cavity and is trapped by the lobes as they rotate. Liquid travels around the interior of the casing in the pockets between the lobes and the casing. Finally, the meshing of the lobes forces liquid through the outlet port under pressure.

Lobe pumps are frequently used in food applications because they handle solids without damaging the product. Since the lobes do not make contact, this design handles low viscosity liquids with diminished performance. Loading characteristics are not as good as other designs, and suction ability is low. High-viscosity liquids require reduced speeds to achieve satisfactory performance. Reductions of 25% of rated speed and lower are common with high-viscosity liquids.

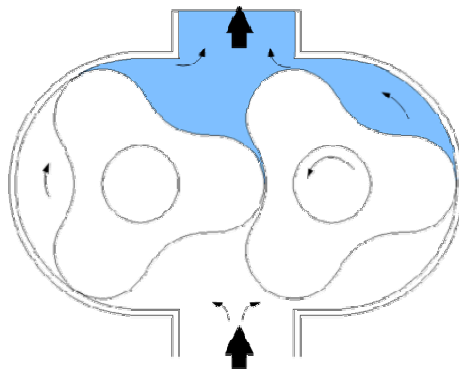


Figure 1-4 Lobe pump [2]

### 3. Screw pump

Screw pumps are a more complicated type of rotary pumps, featuring two screws with opposing thread, as shown in Fig. 1-5, one screw turns clockwise, and the other counterclockwise. The screws are each mounted on shafts that run parallel to each other; the shafts also have gears on them that mesh with each other in order to turn the shafts together and keep everything in place. As with other forms of rotary pumps, the clearance between moving parts and the pump's casing is minimal. As shown in Fig. 1-5, liquid fills the space between adjacent lobes, and as the rotors mesh liquid is trapped between the rotors and the casing. Rotation reduces the space occupied by the gas causing compression, and compression continues until the space becomes exposed to the outlet port through which the liquid is discharged [3].

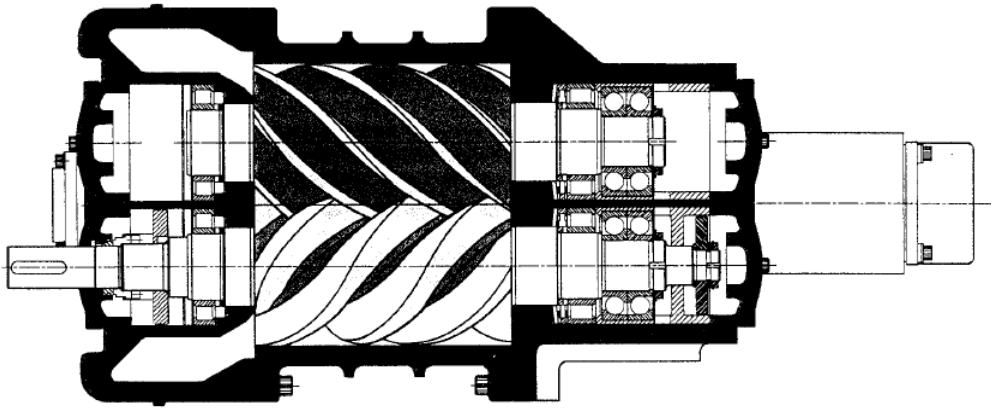


Figure 1-5 Screw pump [3]



Figure 1-6 Operation process of a screw pump [3]

Table 1-1 Comparison of common rotary pumps

	Advantages	Disadvantages
Gear pump	<ol style="list-style-type: none"> <li>1. High head pressure</li> <li>2. High rotation speed</li> <li>3. Low noise</li> </ol>	<ol style="list-style-type: none"> <li>1. Low flow rate</li> <li>2. Medium solids untransportable</li> </ol>
Lobe pump	<ol style="list-style-type: none"> <li>1. No metal-to-metal contact</li> <li>2. Pass medium solids</li> <li>3. Low-pulsation discharge</li> </ol>	<ol style="list-style-type: none"> <li>1. Requires timing gears</li> <li>2. Reduced lift with thin liquids</li> </ol>
Screw pump	<ol style="list-style-type: none"> <li>1. Low noise</li> <li>2. Low-pulsation discharge</li> <li>3. Low leakage</li> </ol>	<ol style="list-style-type: none"> <li>1. Unsuitable in high pressure condition</li> <li>2. High cost</li> </ol>

### 1.3 Literature and patent review

Single claw rotor was applied for a mechanical pump or compressor with oil and particle free devices, as shown in Fig. 1-7. The claw mechanism is a true compressor and can deliver to atmosphere. The non-contact claw rotors are cylindrical for most of their circumference but have a deep depression followed by a protruding claw over one quadrant. This type of claw rotor can be expanded to double claw as shown in Fig. 1-8. There are four processes in one vacuum cycle: inlet exposed, inlet isolated, exhaust exposed and exhaust isolated, as shown in Fig. 1-9.

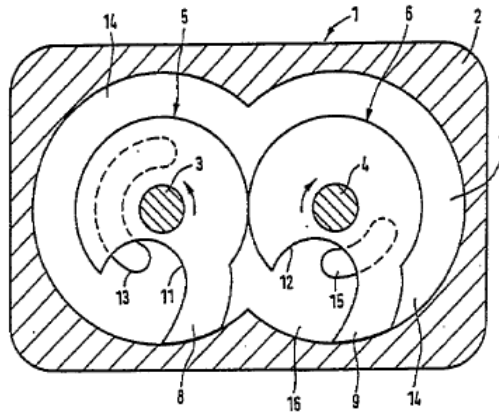


Figure 1-7 Single claw rotor pump in DE19629174 [4]

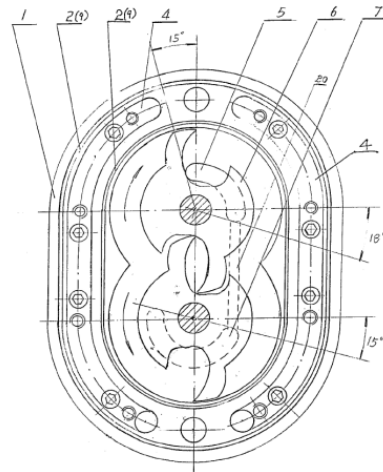


Figure 1-8 Double claw rotor in CN2503232 [5]

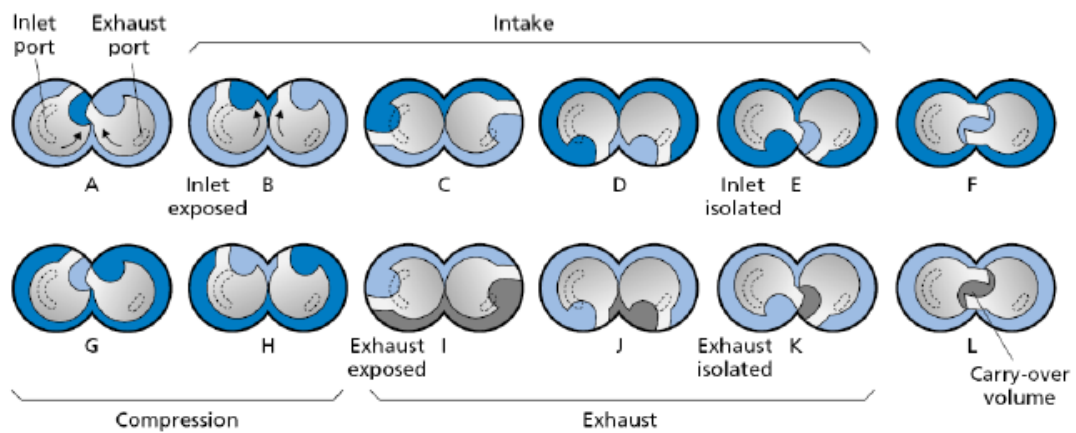


Figure 1-9 Vacuum processes of claw rotor pump [6]

In 2002, a different type single claw rotor was invented by a Chinese company as shown in Fig. 1-10. Rotor contour is designed by involute method. With the same involute method theory, this rotor design can be expanded to double claw, as shown in Fig. 1-11.

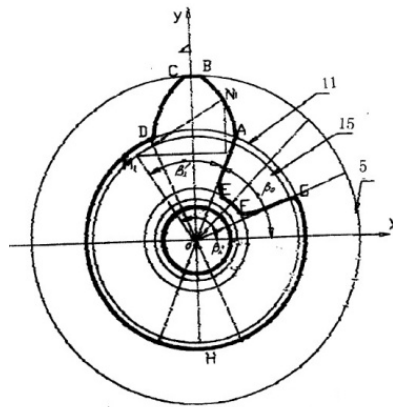


Figure 1-10 Single claw rotor design by involute method [7]

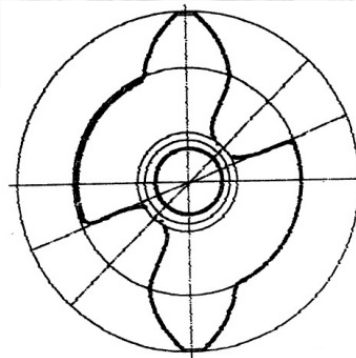


Figure 1-11 Double claw rotor design by involute method [7]

Cycloid method has been widely used in conjugate curve drawing. By this method, claw-shape rotor is connected by a cycloid curve and its envelope curve [5], as shown in Fig. 1-12 and Fig. 1-13.

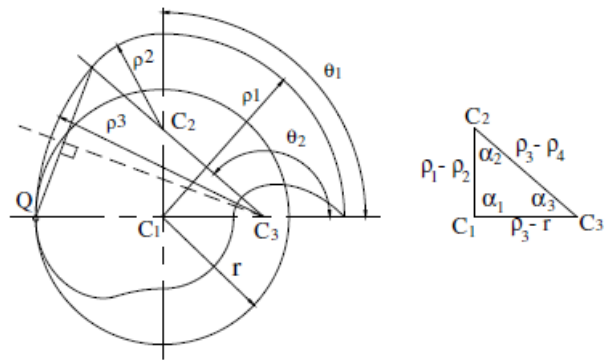


Figure 1-12 Design region of the parameter of 1-claw rotor [8]

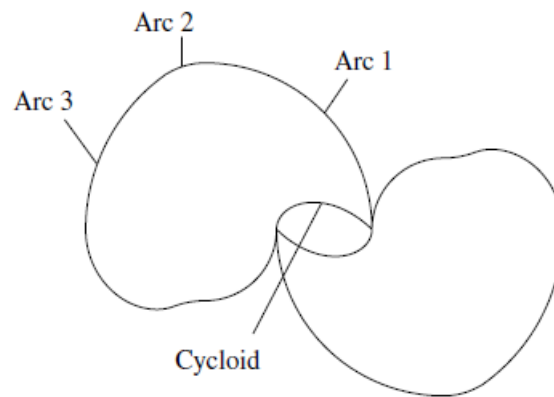


Figure 1-13 1-claw rotor drawn by cycloid method [8]

A German company published a new design of rotary pump with “three blade rotors”, which is a new type 3-claw rotor pump, as shown in Fig. 1-14. This kind of rotor has a totally different contour to the rotors mentioned above, and the volumetric efficiency is higher. An inlet and an outlet which fitted the shape of rotors were also defined on the side wall of the housing chamber.



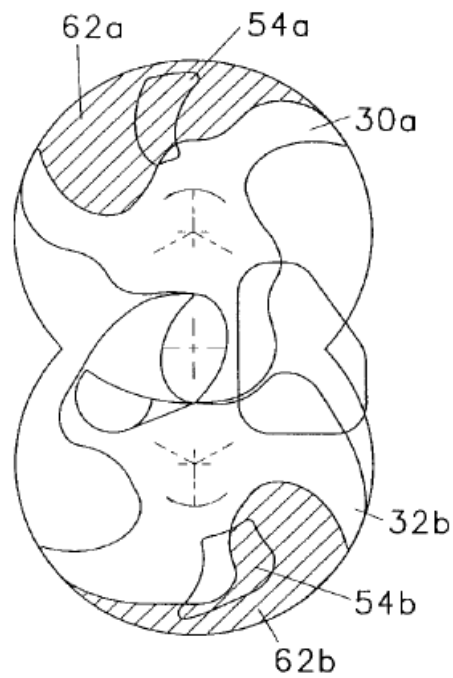


Figure 1-14 3-Claw rotor [9]

During 2004, a new type of compressor using smooth shape 2-claw rotor was invented and this 2-claw rotor design had been planted to pump design during 2006, by Busch LLC, as shown in Fig. 1-15. Moreover, those conjugate rotors can be modified to identical symmetrically-shaped, as shown in Fig. 1-16.

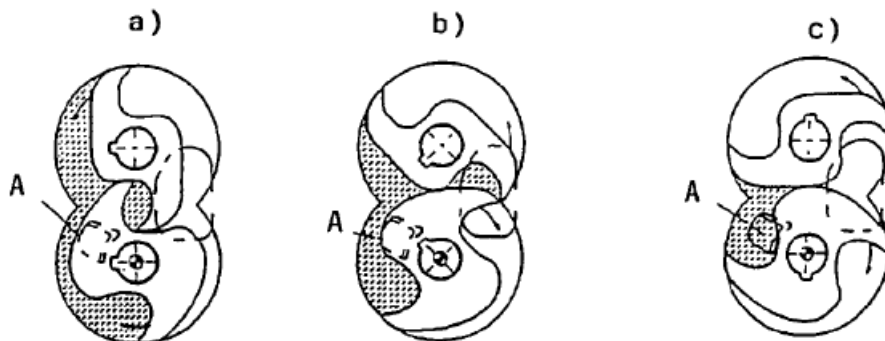


Figure 1-15 Smooth shape 2-claw rotor [10]

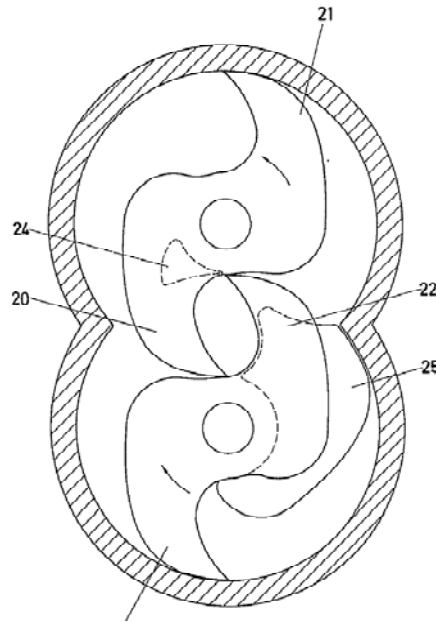


Figure 1-16 Identical symmetrically-shaped 2-claw rotor [11]

Some study claims that claw rotor pump has better performance than other kind of liquid pumps such as centrifugal pump and gear pump. In the condition of high pressure head, the flow rate of centrifugal rapidly decreases and so does its volumetric efficiency, thus centrifugal pump has lower volumetric efficiency than the claw rotor pump does; and gear pump has shorter leakage flow route, in other words the leakage flow in gear pump is greater than in the claw rotor pump, thus the claw rotor pump has better volumetric efficiency than gear pump does [12]. The study also shows that claw rotor pump has higher specific flow rate than gear pump and lobe pump do in the same pitch ratio. Fig. 1-17 is the comparison of specific flow rates of claw rotor, gear and lobe pump in each designate pitch ratio.

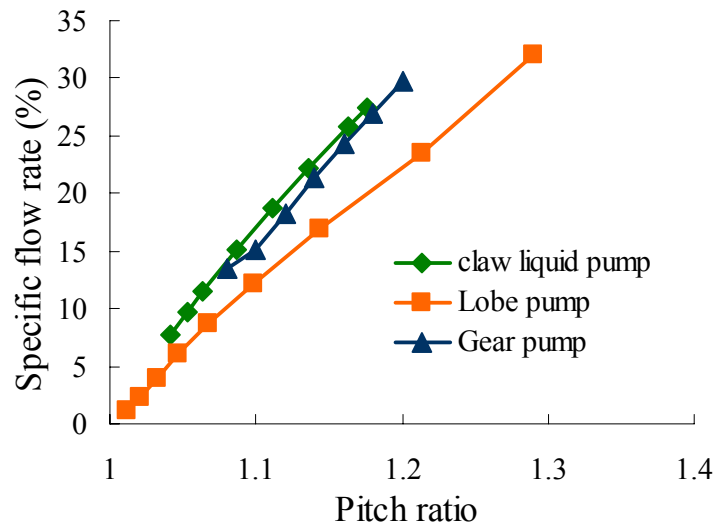


Figure 1-17 Comparison of specific flow rate in designate pitch ratios [12]

One disadvantage with the use of rotary pumps is the unsteady displacement process which produces pressure pulsations, specifically in long and rigid pipelines and non-compressible liquids. The result is vibration of pump and piping, which increases the risk of cavitation on the suction side [13]. The pulsation problem in a three-lobe pump is the result of flow fluctuation, which corresponds to a harmonic vibration, as shown in Fig. 1-18.

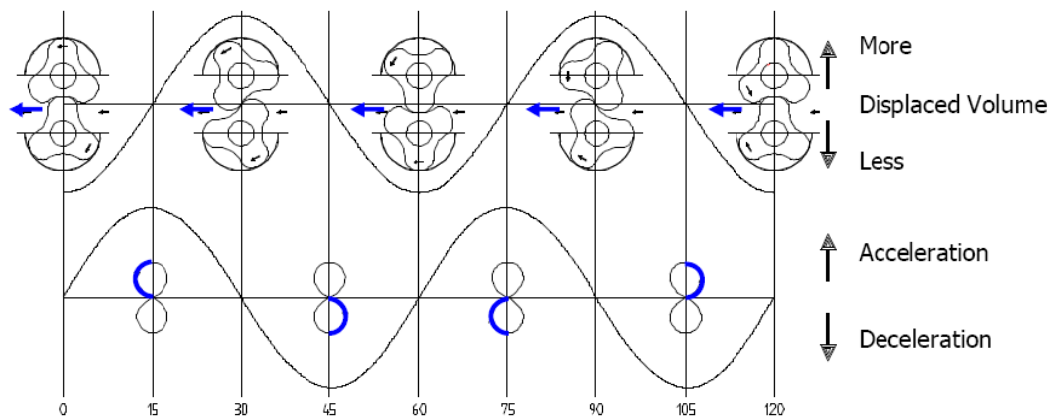


Figure 1-18 Pulsation as the result of flow fluctuation [14]

To solve this pulsation problem, Vogelsang, a German company, proposed the new design of helically toothed lobe pump named “HiFlo” as Germany patent DE19934330085 in 1995, as shown in Fig. 1-19. Every lobe is helically toothed to ensure that the wrap angle along the lobe length is exactly one half of the pitch. This way an indefinite number of minimum partial flow with a uniform, pulsation-free overall flow is achieved within one period. The wrap angle must be an integral number of the half pitch; otherwise the pulsation will not be completely eliminated [13].

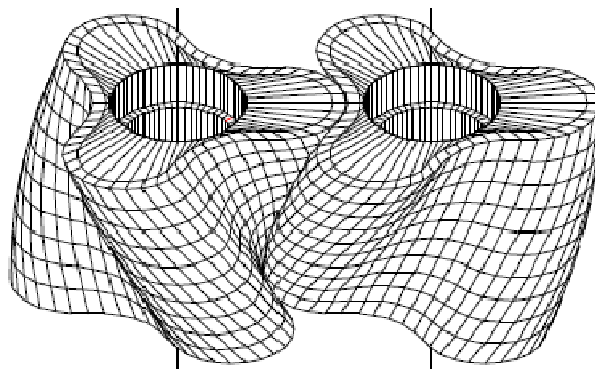
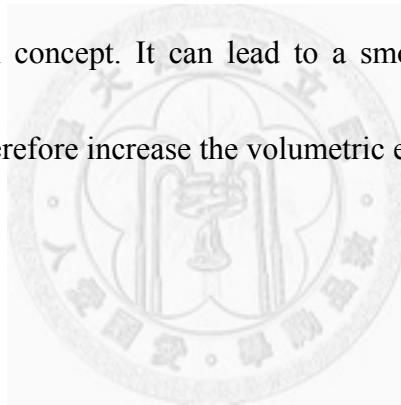


Figure 1-19 Helically toothed lobes [14]

## 1.4 Research objective

According to the literature and patent review, performances of traditional lobe and gear pumps are improved by applying helical design concept. The conventional claw rotor pump has been expected for its characteristics of high pressure head and good volumetric efficiency, and the helical design concept can also be applied to the claw rotor pumps to improve the performance.

The purpose of this thesis is to modify the conventional claw rotor pump by applying the helical design concept. It can lead to a smoother discharge, reduce the pumping fluctuation and therefore increase the volumetric efficiency.



## Chapter 2 Mechanical principles and pump theories

The performance of a rotary pump is commonly examined by the area efficiency and leakage flow in the pump. The area efficiency indicates the volumetric flow rate. Leakage flow denotes the ultimate pressure in the chamber when using a rotary pump.

### 2.1 Specific flow rate and area efficiency

The specific flow rate and area efficiency are defined by the ratio between the volume carried by one rotation and a total chamber volume. When the volume can be represented by the area of the cross-section of the pump, the volumetric efficiency is then discussed by area efficiency.

As the two rotors in a claw rotor pump rotate, a small volume as shown in Fig. 2-1, called carry over, occurs periodically during each compression process. Fluid trapped in the carry over volume will not be discharged, and remains trapped into the next pumping cycle. Consider the carry over volume, the discharge volume per rotation is defined as

$$V_C = (V_{CL} + V_{CR} - V_{CO}) \times N \quad (2.1)$$

where  $V_{CL}$  is the carried volume by left rotor;  $V_{CR}$  is the carried volume by right rotor;

$V_{co}$  is the carry over volume;  $N$  is the number of claws.

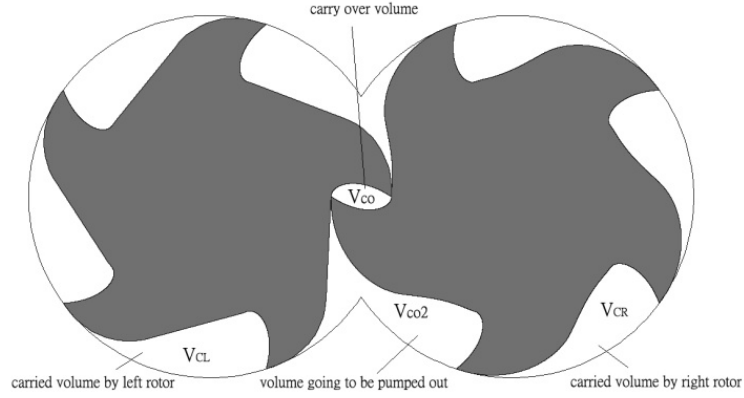


Figure 2-1 Carry over volume of the claw rotor pair

The total volume of the chamber housing as shown in Fig. 2-1 is defined as

$$V_s = \left\{ \pi R_r^2 \frac{\pi - \cos^{-1}(R_p / R_r)}{\pi} + R_r R_p \sin[\cos^{-1}(R_p / R_r)] \right\} \times \delta \quad (2.2)$$

where  $\delta$  is the thickness of the claw rotor pair. The specific flow rate of this claw rotor pump is defined as

$$Q_s = \frac{V_c}{V_s} \quad (2.3)$$

And the specific flow rate of this claw rotor pump is identical to the area efficiency,

which is defined as

$$\eta_A = \frac{A_{cc}}{A_{cs}} = \frac{A_{cc} \times \delta}{A_{cs} \times \delta} = \frac{V_c}{V_s} = Q_s \quad (2.4)$$

where  $A_{cc}$  is the discharge area per rotation and  $A_{cs}$  is the total area of the chamber housing.

## 2.2 Leakage theory

Leakage flow and gap flow are also called clearance flow. In fluid dynamics technology, there should be some clearance between the piston and the cylinder in order to mach up. The clearance between the inner cylinder and the outside piston would cause a gap flow [15], as shown in Fig. 2-2. Calculation formula of gap flow is shown as:

$$q_p = \frac{\pi D_p h^3}{12\mu L} \Delta p \quad (2.5)$$

where  $q_p$  is the quantity of leakage of the piston pump,  $D_p$  is the diameter of the piston,  $h$  is the gap,  $\mu$  is the viscosity coefficient of the fluid,  $L$  is the piston length and  $\Delta p$  is the difference between the pressure head of both end.

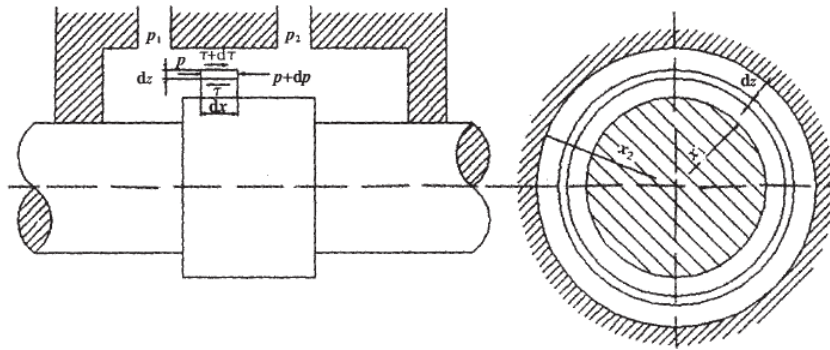


Figure 2-2 Schematic of clearance flow [14]



In a gear pump, the internal fluid would leak through the gap of circuit from the low pressure position to the high pressure position. Base on some leakage theory study, the calculation of leakage flow is generally determined by the gap between the gear top and the stator, and according to fluid dynamic theory [16], the leakage flow can be obtained as:

$$\Delta Q = \frac{b \delta_{gap}^3 \Delta P}{12 \mu \ell_l} \quad (2.6)$$

where  $b$  is the width of gear,  $\delta_{gap}$  is the gap width,  $\Delta P$  is the difference between the inlet and outlet pressure head,  $\mu$  is the viscosity coefficient and  $\ell_l$  is the length of leakage flow route. This theory formula would measure actual leakage flow from the gap between the gear top and the stator of a gear pump.

## 2.3 Pump efficiency

The overall efficiency of a pump is the product of the volumetric efficiency and mechanical efficiency [17-19], and is also defined as the ratio of the power output to the power input. Volumetric efficiency  $\eta_v$  refers to the percentage of actual fluid flow out of the pump compared to the flow out of the pump without leakage (the inlet flow).

Volumetric efficiency is defined as

$$\eta_v = \frac{V_i - V_l}{V_i} = \frac{V_d}{V_i} \quad (2.7)$$

where  $V_i$  is the inlet flow,  $V_l$  is the leakage flow and  $V_d$  is the discharge volume.

Mechanical efficiency is the ratio of the power transmitted by the inlet flow to the power input by the driving shaft,

$$\eta_m = \frac{W_o}{W_{in}} = \frac{\Delta p \cdot V_i}{T \omega} \quad (2.8)$$

where  $W_o$  is the power transmitted by the inlet flow,  $W_{in}$  is the power input by the driving shaft.

The overall efficiency  $\eta_t$  is therefore defined as

$$\eta_t = \eta_v \times \eta_m \quad (2.9)$$

$$\eta_t = \frac{\Delta p \cdot V_d}{T \omega} \quad (2.10)$$

where  $\Delta p$  is the difference between the pressure heads in the outlet port and inlet port,

$T$  is the torque input and  $\omega$  is the angle velocity of the driving shaft.

## Chapter 3 Modified designs of the claw rotor pump

### 3.1 Fundamental of the claw rotor pump

The claw rotor pump is formed with a pair of claw rotors, a pair of timing gears, a pair of shafts and a housing chamber, and the design of the claw rotor pair determines the efficiency of the pumping process.

The left claw rotor is the driving rotor. The contour of an N-claw driving rotor can be separated into N identical claws, composed of 3 arcs, namely arc A, arc B and arc C, 1 line, namely line D, and 1 curve, namely curve F, shown as Fig. 3-1.

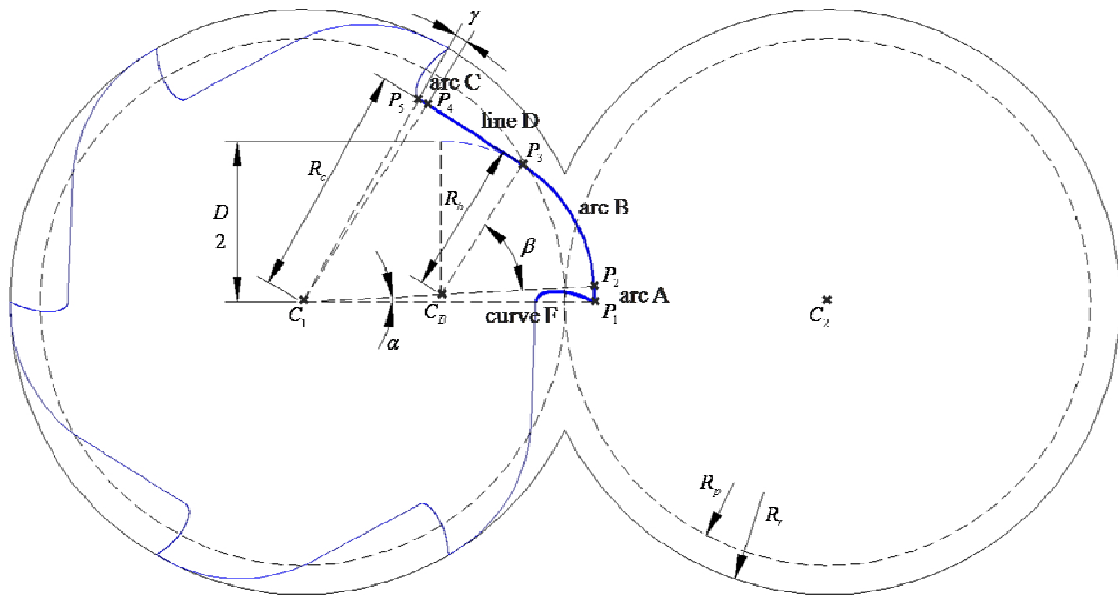


Figure 3-1 Parameters of the driving rotor

The claw's geometry is defined by four significant parameters, namely rotor radius  $R_r$ , pitch circle radius  $R_p$ , depth of claw  $D$  and angle  $\alpha$  of an arc A. Rotor radius  $R_r$  represents the outer radius of rotor. Pitch circle radius  $R_p$  is the radius for drawing the conjugate curve. Depth of rotor  $D$  defines radial depth of the claw. The contact length between a rotor and the stator is decided by angle  $\alpha$ . The parameters of the driving rotor need to be decided firstly, and then the driven rotor is set to be the conjugate curves of the driving rotor. The detailed procedure for producing a pair of claw rotors is described as following.

The center of driving rotor is point  $C_1$  and is also the center of arc A. Arc A starts from point  $P_1$  to point  $P_2$  with radius  $R_r$ . The angle of  $\angle P_1 C_1 P_2$  is equal to angle  $\alpha$ . Arc B is centered at point  $C_B(x_b, y_b)$  with radius  $R_b$  and starts from point  $P_2$  to point  $P_3$ , and the angle of  $\angle P_2 C_B P_3$  is equal to angle  $\beta$ . The relationship between radius  $R_b$ , the depth of claw  $D$ , rotor radius  $R_r$  and angle  $\alpha$  can be defined as following equations:

$$R_b + (R_r - R_b) \sin \alpha = \frac{D}{2} \quad (3.1)$$

$$R_b = \frac{D/2 - R_r \sin \alpha}{1 - \sin \alpha} \quad (3.2)$$

$$\begin{cases} x_b = (R_r - R_b) \cos \alpha \\ y_b = (R_r - R_b) \sin \alpha \end{cases} \quad (3.3)$$

Line D is the common tangent of arc B and arc C, and the tangent point to arc B is point  $P_3$ , and to arc C is point  $P_4$ . The center of arc C is also point  $C_1$ , and arc C starts from point  $P_4$  to point  $P_5$ , and the angle of  $\angle P_4 C_1 P_5$  is equal to angle  $\gamma$ . Angle  $\beta$  and angle  $\gamma$  can be derived by geometric methods, thus the coordinates of tangent points  $P_3$  and  $P_4$  are determined.

$$R_c = 2R_p - R_r \quad (3.4)$$

$$\beta = \cos^{-1} \frac{R_c - R_b}{\sqrt{x_b^2 + y_b^2}} \quad (3.5)$$

$$\gamma = \frac{360^\circ}{N} - (\alpha + \beta) \quad (3.6)$$

Curve F is the conjugate curve of the claw tip of the right rotor, and the conjugate curve generating process is shown as Fig.3-2. The point of the claw tip of right rotor rotates (step 1) about the center of right rotor in the rotation angle  $\varphi$  from  $0^\circ$  to  $\cos^{-1}(R_p / R_r)$  clockwise to get the transition point (step 2), and then rotates this point about the center of left rotor in  $\varphi$  counter-clockwise to get the conjugate point of the claw tip (step 3). Finally, curve F is obtained by linking conjugate points of all rotation angles together.

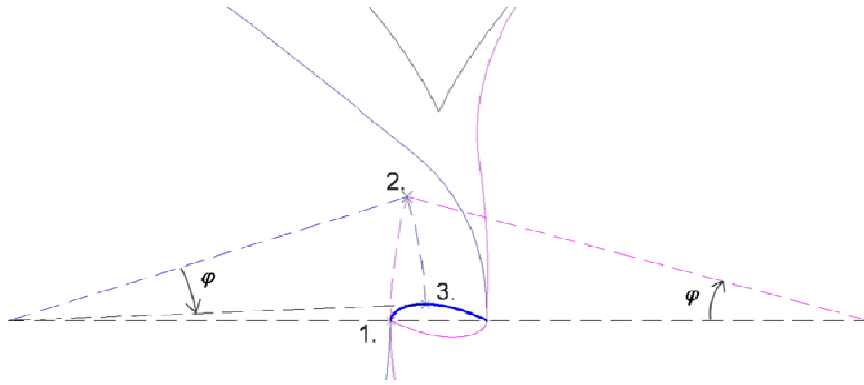
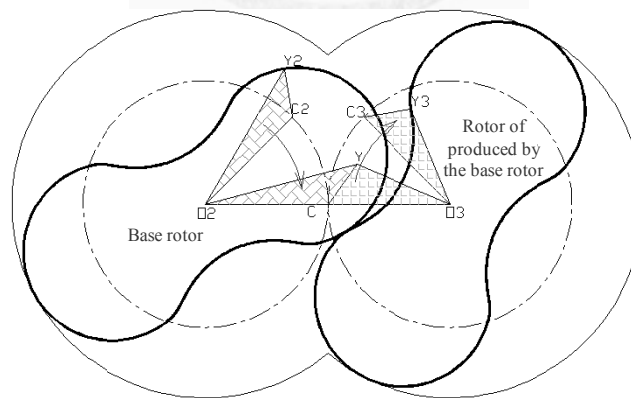
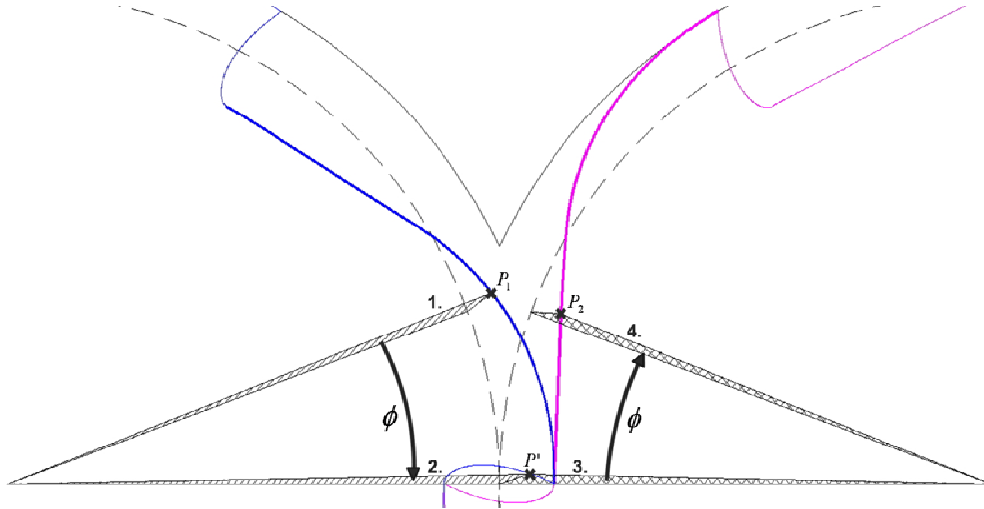


Figure 3-2 Generating process of curve F

The contour of the right rotor, which is the driven rotor, is the conjugate curve of the left rotor, and the conjugate curve generating process is similar to the rotor pair of lobe pump, shown as Fig. 3-3. The claw rotor pair defined by this method has two distinct rotors, in other words, the driving rotor and the driven rotor are different in shapes.



(a) Conjugate curve generating process of the lobe rotor pair [20]



(b) Conjugate curve generation process of the claw rotor pair

Figure 3-3 Generating process of the right rotor

The claw rotors' contours can be set into parametric model. Set the center of left rotor as the coordinate origin, and define the distance from the origin to a point on left rotor's contour as a function of angular coordinate  $\theta$ , as shown in Fig. 3-4.

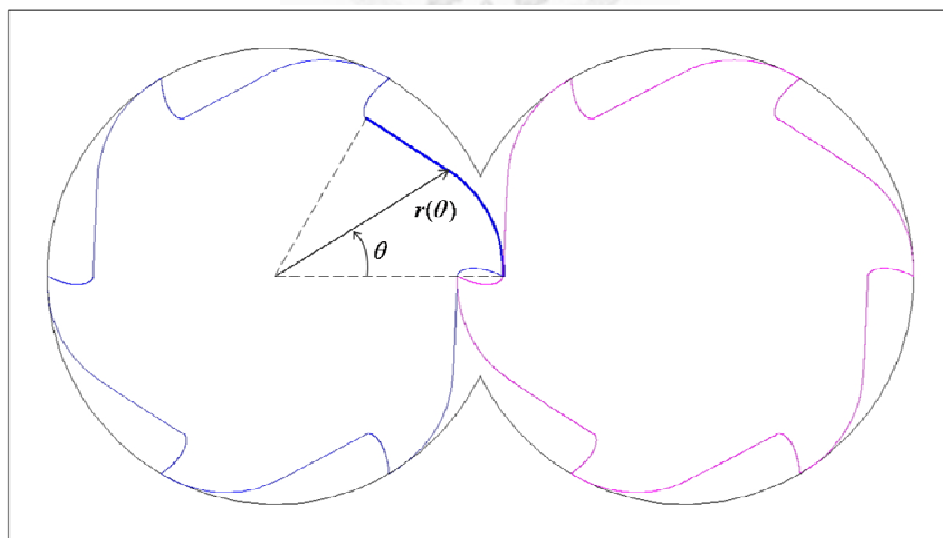


Figure 3-4 Distance function of angular coordinate  $\theta$

The distance function  $r(\theta)$  can be derived by the claw geometry. When

$$0^\circ \leq \theta < \alpha,$$

$$r(\theta) = R_r \quad (3.7)$$

$$\text{when } \alpha \leq \theta < \tan^{-1} \frac{b_y}{b_x},$$

$$r(\theta) = x_b \cos \theta + y_b \sin \theta + \sqrt{f(\theta)} \quad (3.8)$$

$$f(\theta) = (x_b \cos \theta + y_b \sin \theta)^2 - (x_b^2 + y_b^2 - R_b^2) \quad (3.9)$$

$$\text{when } \tan^{-1} \frac{b_y}{b_x} \leq \theta < \beta,$$

$$r(\theta) = \frac{h_D}{\sin \theta - m_D \cos \theta} \quad (3.10)$$

$$\text{and when } \beta \leq \theta \leq \gamma,$$

$$r(\theta) = R_c \quad (3.11)$$

So the parameterization of the left rotor's contour is therefore defined as

$$\begin{cases} x = r(\theta) \cos \theta \\ y = r(\theta) \sin \theta \end{cases} \quad (3.12)$$

Then the parametric model of the right rotor's contour can also be defined by the conjugate curve's geometry, and the needed parameters are shown in Fig. 3-5.



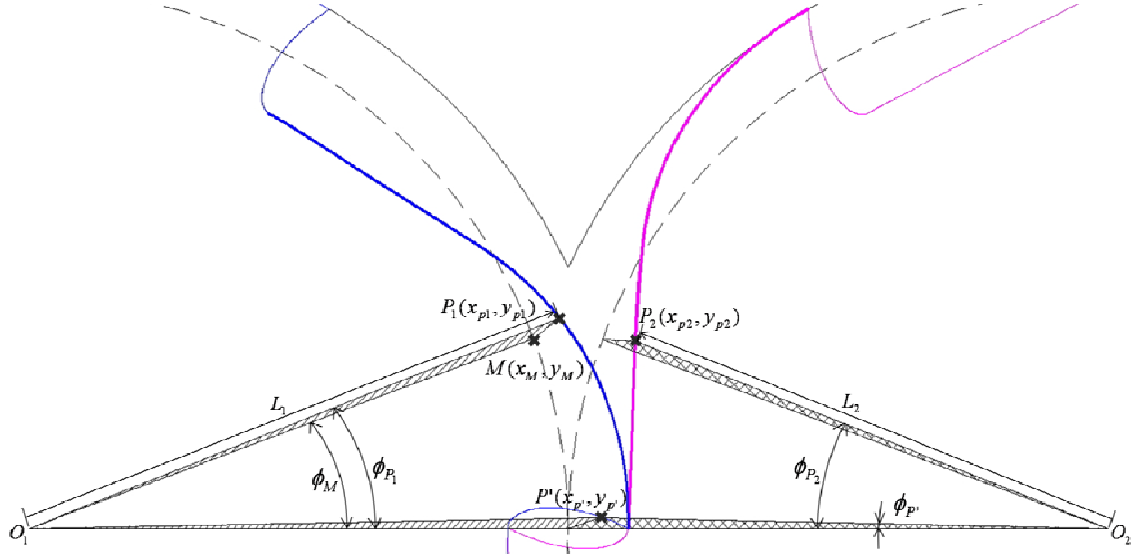


Figure 3-5 Parameters for the generation of the conjugate rotor

For every point  $P_1$  in the left rotor's contour, there is a conjugate point  $P_2$  corresponding in the right rotor. First, the normal of  $P_1$  intersects the pitch circle of the left rotor at point  $M$ , and the coordinate of point  $M$  is derived as

$$\begin{cases} x_M = \frac{g(\theta) + \sqrt{g^2(\theta) - h(\theta)}}{2(1 + m_N^2)} \\ y_M = m_N(x_M - x_{p1}) + y_{p1} \end{cases} \quad (3.13)$$

$$g(\theta) = 2m_N(m_N x_{p1} - y_{p1}) \quad (3.14)$$

$$h(\theta) = 4(1 + m_N^2)[(y_{p1} - m_N x_{p1})^2 - r_p^2] \quad (3.15)$$

where  $m_N$  is the slope of the normal. Then, rotate the triangle about the center of left rotor  $O_1$  in  $\phi_M$  to obtain point  $P'$ ,

$$\begin{cases} x_{p'} = L_1 \cos(\phi_{P_1} - \phi_M) \\ y_{p'} = L_1 \sin(\phi_{P_1} - \phi_M) \end{cases} \quad (3.16)$$

and then rotate the new formed triangle about the center of right rotor  $O_2$  in  $\phi_M$  to obtain the conjugate point  $P_2$  [21].

$$\phi_{P_2} = \phi_M + \phi_{p'} \quad (3.17)$$

$$\begin{cases} x_{p2} = 2R_p - L_2 \cos \phi_{P_2} \\ y_{p2} = L_2 \sin \phi_{P_2} \end{cases} \quad (3.18)$$

After the parametric model is constructed, the pumping flow rate, volumetric efficiency and pumping pulsation of the claw rotor pump can be further derived.

### 3.2 Modified designs of the claw rotor

Periodically fluctuation which occurs in the operation process of the rotary displacement pump generates pressure pulsation in the connected piping due to acceleration and deceleration [13]. For example, the internal displacement mechanism of a rotary lobe pump which is designed according to the Roots principle brings about flow fluctuation with a peak value. Similar condition would happen to the claw rotor pump, too.

Moreover, as the development of the claw rotor pump comes to multi-stage design,

the discontinuous flow and the pulsation would become serious problems since the flow rate difference between different stages would cause further vibration and decrease in pump efficiency.

In the thinking of pulsation avoidance, making continuous discharge flow is the key factor of the modified design of claw rotor pump. Inspired by the HiFlo rotor, the helical design is applied to the claw rotors, which is like phase shifting an indefinite number of the cross-sections of the claw rotor pair and superimposing the discharge flow. The helix angle  $\phi_h$  is firstly defined, and then the rotation angle  $\phi$  would be linear to the axial direction  $z$  as shown in Fig. 3-6, so the relation between  $\phi$  and  $z$  is expressed below:

$$\phi(z) = \frac{\phi_h}{\delta} \cdot z \quad (3.19)$$

where  $\phi_h$  is the designed helix angle and  $\delta$  is the thickness of the rotor pair.

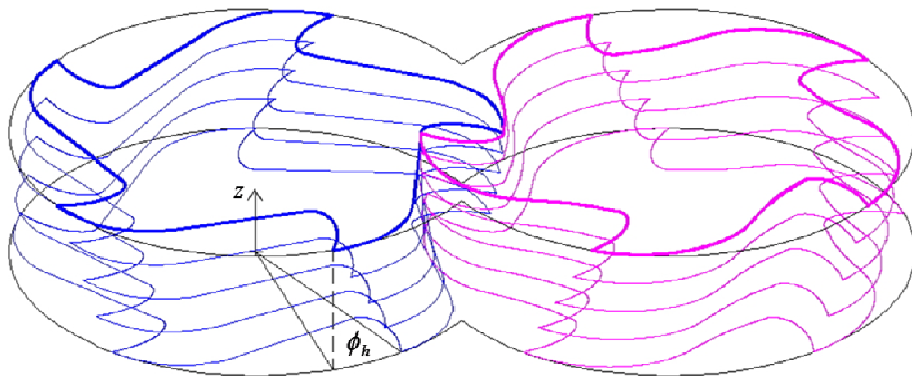


Figure 3-6 Rotation angle is linear to the axial direction

In spite of making continuous discharge flow, the helical claw rotor pump has another advantage which is the longer leakage flow route compared with the conventional design. The helical profile provides longer leakage flow routes in the contact surfaces, which reduce the leakage flow and increase the volumetric efficiency.

A designed 5-claw helical claw rotor pair is shown in Fig. 3-7 and Fig. 3-8.

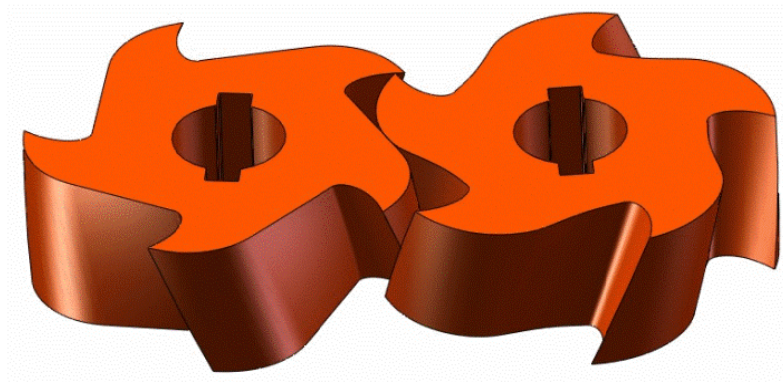


Figure 3-7 Solid model of the helical claw rotor pair

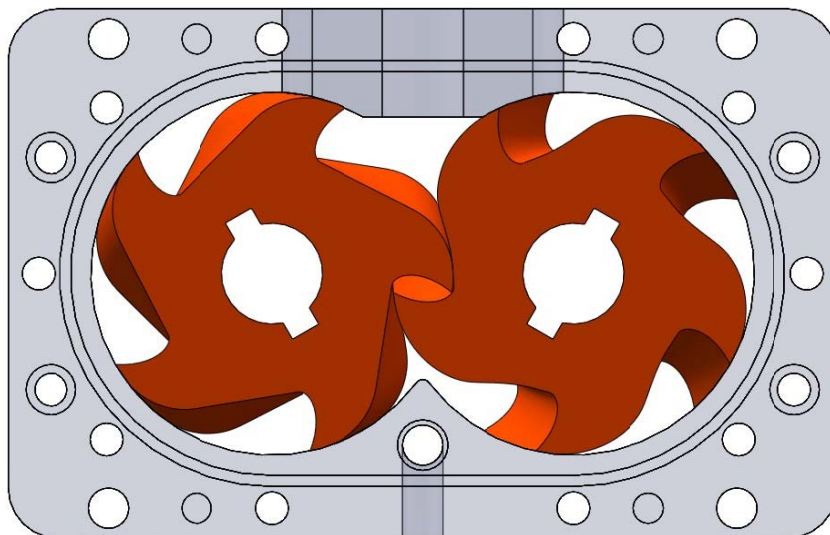
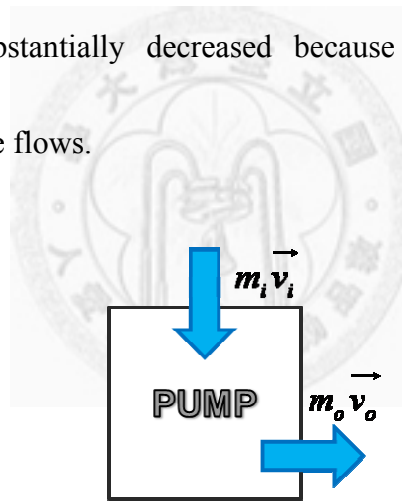
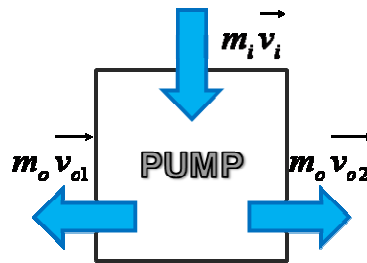


Figure 3-8 Helical claw rotors in the housing chamber

As shown in Fig. 3-9(a), the momentum of the inlet volume enters the pumping chamber from the vertical direction, and the output volume discharges to the helical direction. There must be forces act on the pumping chamber to balance the momentum of the system, and those forces are supplied by rotors, bearings and shafts. Reaction forces due to the one-way flow exert on rotors, bearings and shafts would cause fatigue and damage, and that is a drawback of the helical claw rotor pump. Considering a two-way discharging process, as shown in Fig. 3-9(b), the force needed to balance the system momentum is substantially decreased because of the offset of the two opposite-direction discharge flows.



(a) Unidirectional discharge



(b) Two-way discharge

Figure 3-9 System momentum of the claw rotor pump

In order to make the discharge flows export to two opposite directions, the helical design should be modified. The concept is to modify the profile line of the helical claw rotor to a curve shape, as the curve formed by rolling up a plane with an arc on it to a cylinder. This concept is similar to the helical design, and there is also a helix angle  $\phi_h$  which means the largest phase shifting angle. The curve-sided shape of claw rotor is obtained by rotating the claw rotor cross-section about its axial while extruding it to a solid model, and the relation between the rotation angle  $\phi$  and the axial direction  $z$  can be obtained by geometric methods, as shown in Fig. 3-10, and is expressed below:

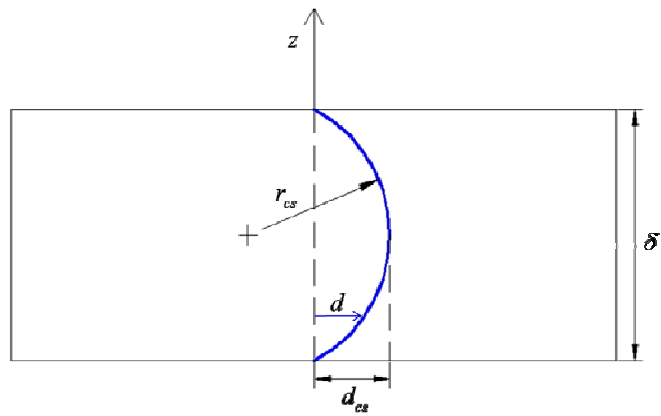
$$d_{cs} = R_r \cdot \phi_h \quad (3.20)$$

$$r_{cs} = \frac{4d_{cs}^2 + \delta^2}{8d_{cs}} = \frac{4R_r^2 \phi_h^2 + \delta^2}{8R_r \phi_h} \quad (3.23)$$

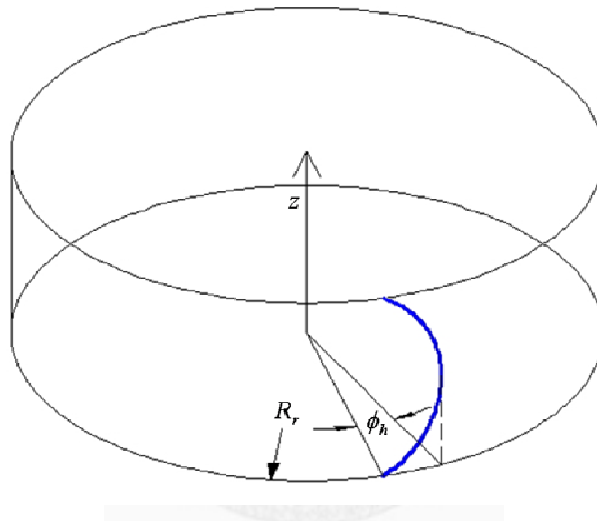
$$d = R_r \phi_h - r_{cs} + \sqrt{r_{cs}^2 - (\delta/2 - z)^2} \quad (3.21)$$

$$\phi(z) = \frac{d}{r_{cs}} = \frac{R_r \phi_h - r_{cs} + \sqrt{r_{cs}^2 - (\delta/2 - z)^2}}{r_{cs}} \quad (3.22)$$

And the solid model of this new designed curve-sided type helical claw rotor pair is therefore obtained and is shown in Fig. 3-11.



(a) Designed arc on a plane and its variables



(b) Rolling up the plane to a cylinder

Figure 3-10 Curve formed by rolling up a plane with an arc on it to a cylinder

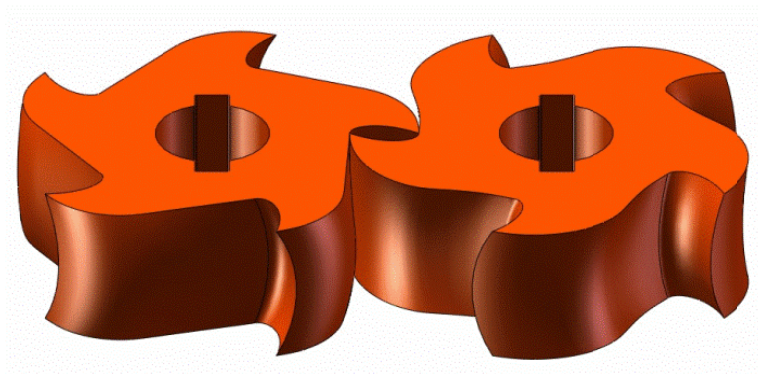
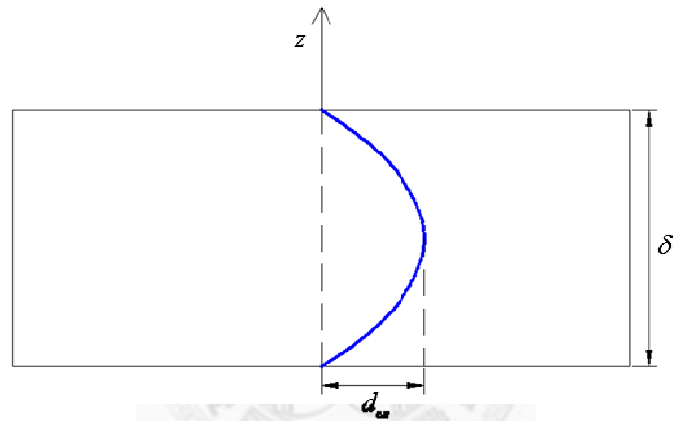
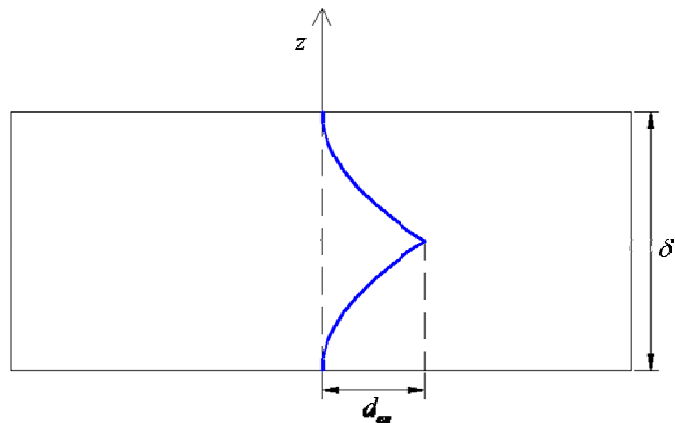


Figure 3-11 Solid model of the curve-sided type helical claw rotor pair

For the same design concept, the curve-sided shape can be adjusted, for example, from an arc on a plane to a parabola on a plane or even a yoke shape curve on a plane, as shown in Fig. 3-12, and two new types of curve-sided type helical claw rotor pumps are created, namely parabolic curve-sided and yoke shape curve-sided type helical claw rotor pump, as shown in Fig. 3-13.



(a) Designed parabola on a plane and its variables



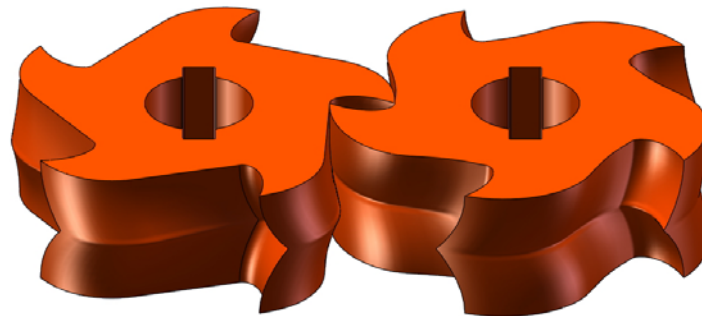
(b) Designed yoke shape on a plane and its variables

Figure 3-12 Curve shapes on a plane





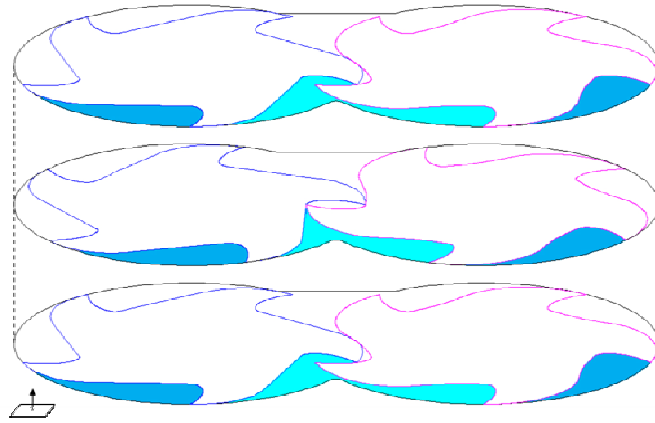
(a) Parabolic curve-sided type



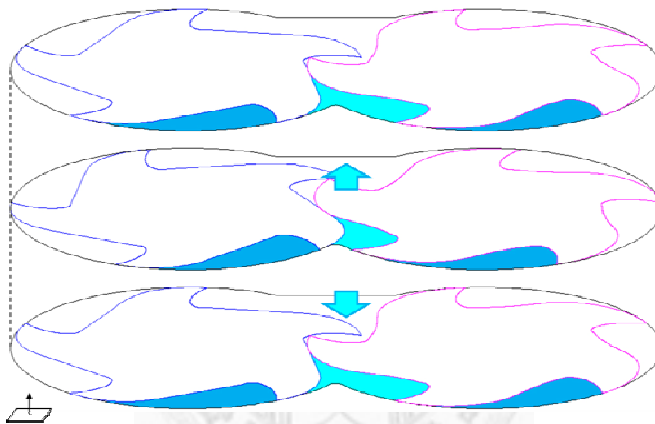
(b) Yoke shape curve-sided type

Figure 3-13 Two curve-sided type helical claw rotor pairs

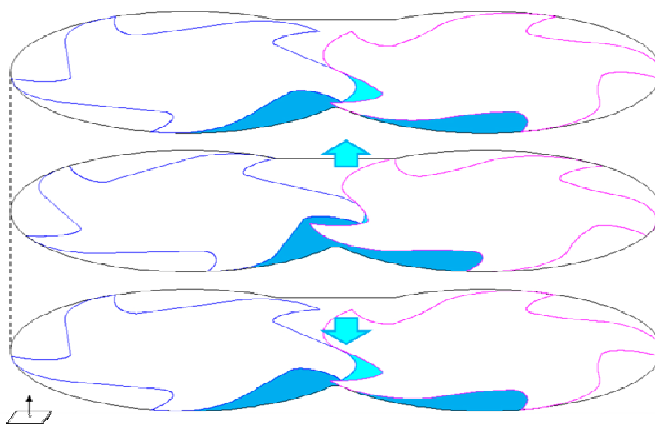
The main idea of the curve-sided helical design is to make the discharge flow export from the middle part of the rotor pair to both sides. As the rotor pair rotates, the fluid would be sucked into the inlet port and carried to the extruding area, and the middle part of the rotor pair is the leading face, and the side parts are the lagging faces, so the fluid volume in the middle part of the extruding area would be extruded to both sides. Fig. 3-13 shows the pumping process described above by decomposing every rotor to three cross-sections, so the discharge flow to both up and down side at the same time can be observed distinctly.



(a) Discharge process for angular position at 0 degree



(b) Discharge process for angular position at 30 degree



(c) Discharge process for angular position at 60 degree

Figure 3-14 Discharge process of the curve-sided helical claw rotor pump

## **Chapter 4**

### **Performance analysis of the claw rotor pump**

The specific flow rate of the claw rotor pump has been proved higher than of gear and lobe pump, and some experiments also showed the outstanding characteristic of high volumetric efficiency and pressure head, mentioned in chapter 1 of this thesis, but the instantaneous flow rate and fluctuation analysis of the claw rotor pump still have never been researched. In this chapter, a computer program would be created to analyze the volumetric flow rate per designate rotation angle, hence the condition of flow fluctuation is therefore obtained. The claw rotor pump and its modified designs, namely helical claw rotor pump and curve-sided type helical claw rotor pump, are analyzed by the program and compared with each other.

#### **4.1 Volumetric flow rate calculation**

The fluid volume in the pump is the deduction of the rotor volumes from the chamber volume, so as long as the area of the rotors' contour is calculated, the fluid volume is therefore obtained. By parametric programming, the relation between the angular position of the rotor pair and the instantaneous flow rate can be derived.

The claw rotor pump is formed with a pair of claw rotors, a pair of timing gears, a pair of shafts and a housing chamber, and the design of the claw rotor pair determines the efficiency of the pumping process.

During a pumping process, the carried volumes of both rotors enter the extruding area. As shown in Fig. 4-1, the fluid volume (hatched areas), which is the subtraction between the chamber volume (two sector areas) and the rotor volume (dark area), can be calculated since the parametric model is created, and the derivation is expressed below:

$$A_{i,left} = \int_0^{\theta_i} \frac{1}{2} r^2(\theta) d\theta \quad (4.1)$$

$$A_{i,fluid} = A_{i,chamber} - (A_{i,left} + A_{i,right}) \quad (4.2)$$

where  $i$  is the ID number representing the instantaneous angular position of the rotor pair,  $\theta_i$  stands for the interval from the claw tip to the contact point of two rotors, and the area of right rotor  $A_{i,right}$  is derived by integration program, which separates the rotor into small triangles and sum up the areas, as shown in Fig.4-2.

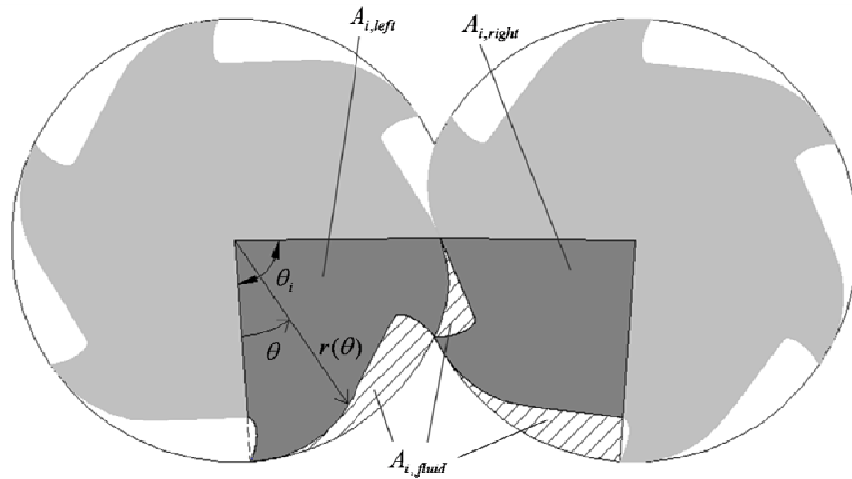


Figure 4-1 Fluid volume is the subtraction between chamber volume and rotor volume

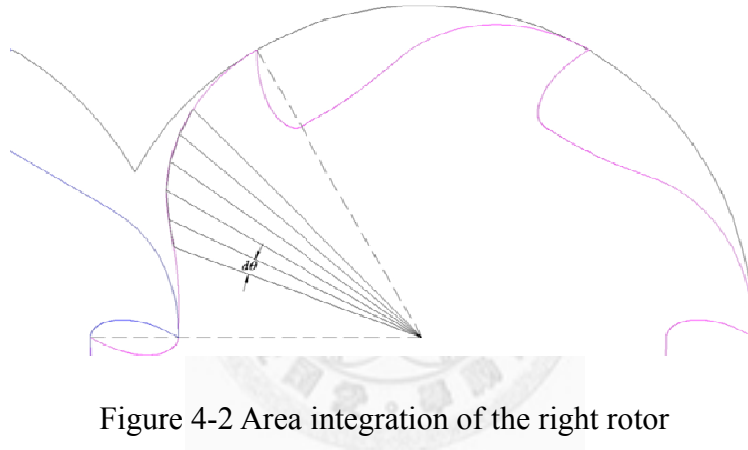


Figure 4-2 Area integration of the right rotor

As the cross-section area of the fluid in any designate angular position is derived, the fluid volume can be therefore obtained by integrating the area along the axial direction, and Fig. 4-3 is an example shown in a helical claw rotor pair.

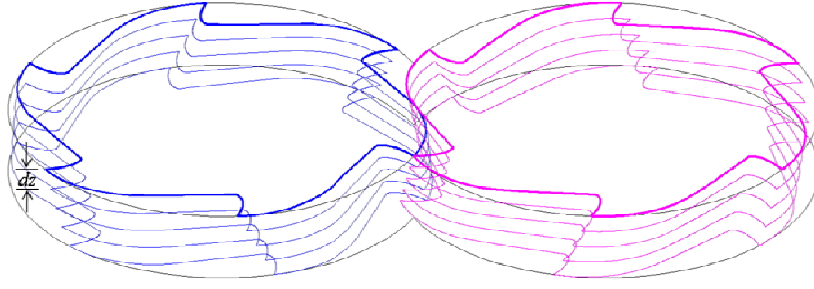


Figure 4-3 Derivation for the fluid volume of the helical claw rotor pump

For the conventional claw rotor pump, the fluid volume is simply the product of the cross-section area of fluid  $A_{i,fluid}$  and the rotor thickness because the helical angle is 0 degree.

$$V_i = A_{i,fluid} \cdot \delta \quad (4.3)$$

For the helical claw rotor pump, the rotation angle  $\phi$  is linear to the axial direction  $z$  as equation (3.19), and the upper limit  $\theta_i$  in equation (4.1) varies with  $\phi(z)$ , so  $\theta_i$  can be expressed as a function of  $z$ . Therefore, equation (4.1) is further derived as

$$A_{i,left}(z) = \int_0^{\theta_i(z)} \frac{1}{2} r^2(\theta) d\theta \quad (4.4)$$

and the cross-section area of fluid  $A_{i,fluid}$  can be also expressed as a function of  $z$ .

The fluid volume of the helical claw rotor pump  $V_i$  is

$$V_i = \int_0^{\delta} A_{i,fluid}(z) dz \quad (4.5)$$

For the same concept the fluid volume of curve-sided type helical claw rotor pump is expressed as equation (4.5), only the upper limit  $\theta_i(z)$ , which means the interval from the claw tip to the contact point of two rotors, is different from the helical claw rotor pump.

The instantaneous flow rate means the variation of fluid volumes between two consecutive angular positions, which represents the volume flow out of the pump during a small angular interval, and is expressed as

$$Q_i = V_i - V_{i+1} \quad (4.6)$$

So the instantaneous flow rate of the claw rotor pump and its modified designs can be therefore derived. A computer program for flow rate calculation is created by Visual Lisp for AutoCAD (namely AutoLISP). The program instruction and lisp code are listed in Appendix A.

## 4.2 Flow rate analysis of the claw rotor pump

During an operation process of the claw rotor pump, pulsation would occur because of the discontinuous flow, and the instantaneous flow rate is calculated by the developed analysis program. As shown in Fig. 4-5, the instantaneous flow rate of a claw rotor

pump is not continuous and has a peak value, but the fluctuation of the discharge flow is different from the lobe pump.

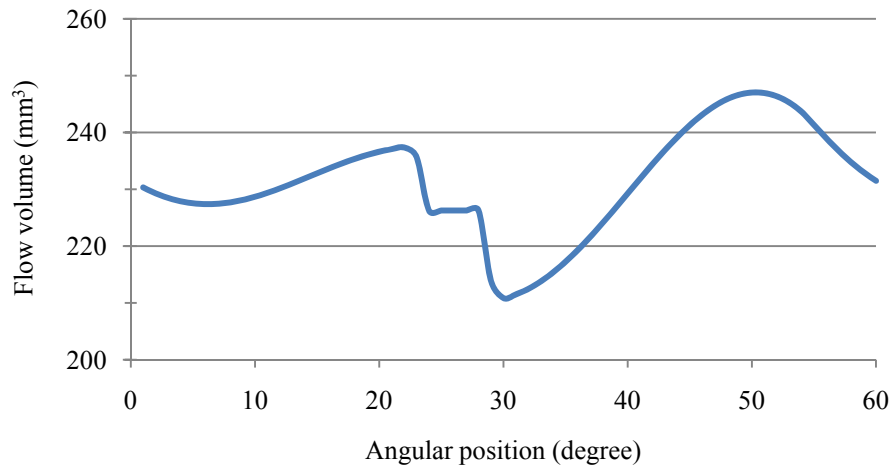


Figure 4-5 Flow rate in 1 period of a 6-claw rotor pump

To figure out what affects the pumping fluctuation form, the number of claws is taken into consideration. As the displacement (i.e. discharge volume per rotation) of the pump is set fixed, a 4-claw, 5-claw and 6-claw claw rotor pairs are then designed in order to compare the difference between flow continuities of claw rotor pumps with different claw numbers. The rotor radius, pitch radius and rotor thickness are also set fixed so the three rotor pairs can be assembled in the same housing chamber. The variables of these claw rotor pairs are listed as Table 4-1, and the comparison of instantaneous flow rates between different claw numbers is shown as Fig. 4-6.



Table 4-1 Design variables of claw rotor pumps

No. of claws	4	5	6
Displacement	83400 mm <sup>3</sup> /rotation		
Rotor radius (mm)	60	60	60
Pitch radius (mm)	54	54	54
Rotor depth (mm)	89	77	66
Alpha angle (degree)	3	3	3
Thickness (mm)	20	20	20

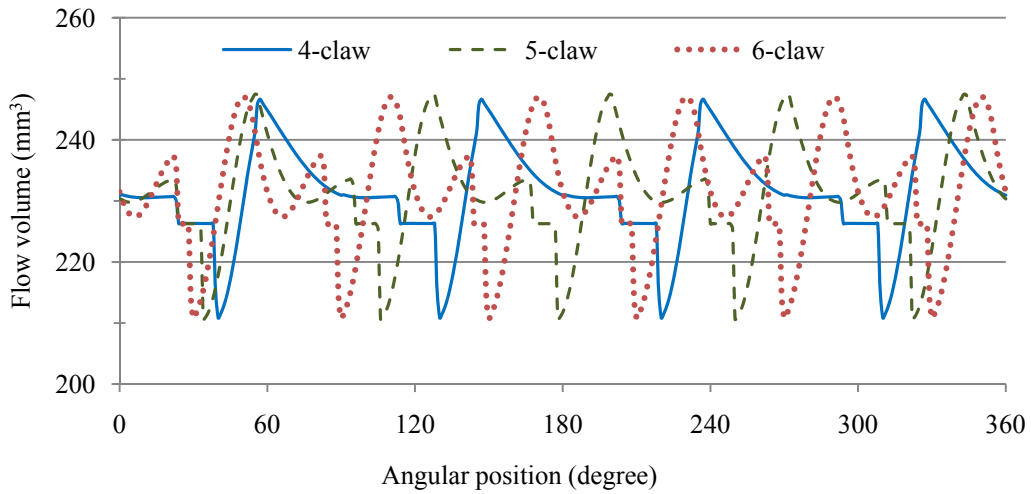


Figure 4-6 Flow rate of pumps with different claw numbers

The flow rate fluctuation coefficient  $\lambda$  is defined as the ratio of the amplitude and the average instantaneous flow rate [22]. The amplitude of the fluctuation represents the difference between the largest and the smallest instantaneous flow rates, and the average instantaneous flow rate means the total flow volume per rotation divided by 360 degree.

As Fig. 4-6 shows, the maximum values and the minimum values of the instantaneous flow rates of the three claw rotor pumps are very close, and the flow rate fluctuation coefficients are listed as Table 4-2.

$$\lambda = \frac{\dot{V}_{\max} - \dot{V}_{\min}}{\dot{V}_{av}} \quad (4.7)$$

Table 4-2 Fluctuation coefficient of different number of claws

No. of claws	4	5	6
$\lambda$	0.1547	0.1593	0.1563

The flow rate fluctuation coefficients tell that the number of claws would not obviously affect the fluctuation during operation process. The flow volume chart Fig. 4-6 tells that waveforms of claw rotor pumps with different number of claws are very similar, so the analysis of the affection by helix angle is then discussed.

### 4.3 Flow rate analysis of the helical claw rotor pump

After the flow volume chart of the claw rotor pump is obtained, different helix angles are applied to the rotor design to analyze the relation between helix angle and the continuity of discharge flow.

Fig. 4-5 and Fig. 4-6 also show the irregularity of the fluctuation of the claw rotor

pump in one period, and that means that the pulsation would not be completely eliminated until the helix angle is an integral number of one pitch. Taken the difficulty of manufacture into consideration, helical claw rotor pairs with the helix angle of one pitch are impractical; moreover, the claw tips would become too sharp and weaken the strength of rotors, so an appropriate helix angle is the emphasis in the helical claw rotor design.

Therefore, seven different helical angles are applied to the 4-claw, 5-claw and 6-claw claw rotor pairs, and by using the analysis program which is developed in this thesis, the flow performances of these 21 design helical claw rotor pumps and the conventional claw rotor pumps are analyzed and compared with each other, as shown in Fig. 4-7 to Fig. 4-9, and the flow rate fluctuation coefficients are listed as Table 4-3 to Table 4-5. The detailed data of the instantaneous flow rates of the helical claw rotors designed in this thesis are listed in Appendix B.

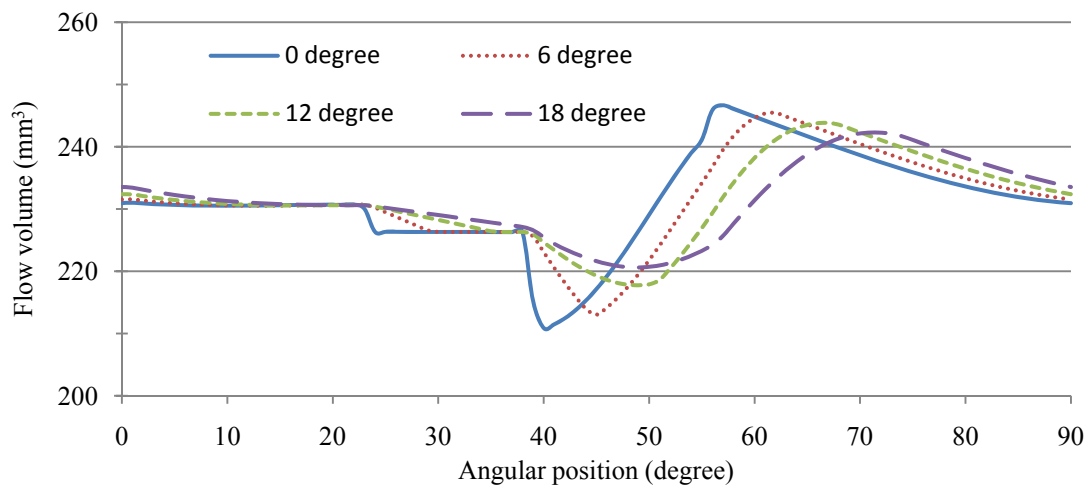


Figure 4-7 Flow rate of the 4-claw helical rotor pump

Table 4-3 Fluctuation coefficients of the 4-claw helical rotor pump

No. of claws	Helix angle	$\lambda$
4	0°	0.1547
	3°	0.1506
	6°	0.1400
	9°	0.1264
	12°	0.1127
	18°	0.0937
	24°	0.0812
	30°	0.0694

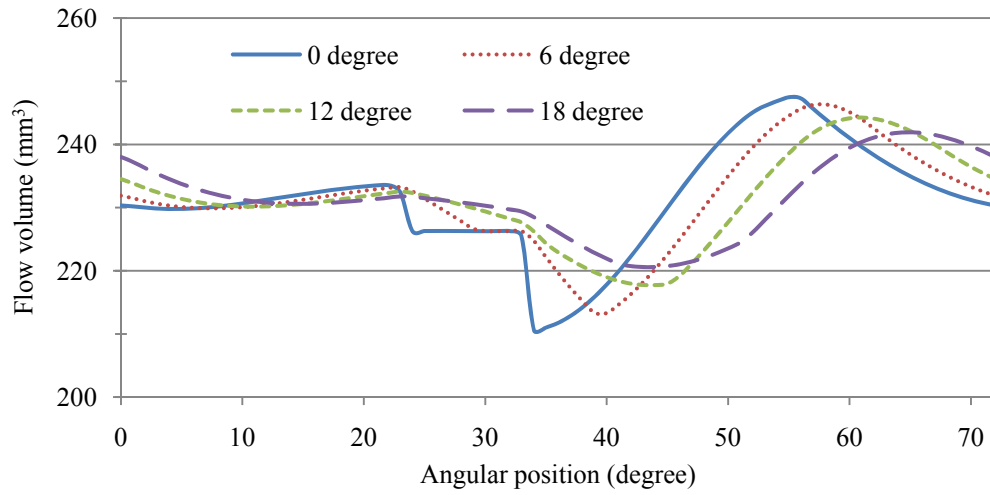


Figure 4-8 Flow rate of the 5-claw helical rotor pump

Table 4-4 Fluctuation coefficients of the 5-claw helical rotor pump

No. of claws	Helix angle	$\lambda$
5	0°	0.1593
	3°	0.1540
	6°	0.1428
	9°	0.1303
	12°	0.1146
	18°	0.0923
	24°	0.0735
	30°	0.0572

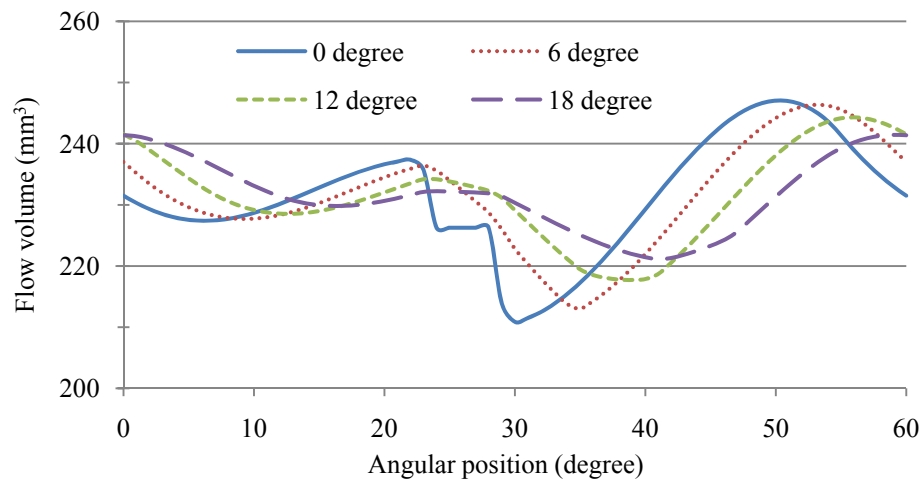


Figure 4-9 Flow rate of the 6-claw helical rotor pump

Table 4-5 Fluctuation coefficients of the 6-claw helical rotor pump

No. of claws	Helix angle	$\lambda$
6	0°	0.1563
	3°	0.1534
	6°	0.1440
	9°	0.1301
	12°	0.1149
	18°	0.0879
	24°	0.0599
	30°	0.0442

The analysis shows that helix angle is the key factor to make the discharge flow more continuous, and as the helix angle increases, the discharge flow would become more continuous, thus could decrease the pulsation during the pump operation process.

The analysis also reveals that as the claw number increases, the helix angle would become more effective in pulsation reduction. That is due to the period decrease while the increase in claw number, in other words, the proportion would account larger in a smaller period for the same helix angle. For example, a  $18^\circ$  helix angle can completely eliminate the flow fluctuation of a 20-claw claw rotor pump while the fluctuation coefficient is 0.0879 in a 6-claw claw rotor pump.

People can choose the proper helix angle to meet their intention by the design process described in this thesis.

#### **4.4 Flow rate analysis of the curve-sided type helical claw rotor pump**

By using the analysis program developed in this thesis, the instantaneous flow rate of a curve-sided type helical claw rotor pump can be predicted. Because of its geometry, the curve-sided type helical claw rotor pair has a maximum value which depends on the rotor radius and thickness, and the maximum value is  $9^\circ$  in this design. Three different

curve-sided type helical claw rotor pairs with different helix angles are designed and analyzed, and the comparison chart of flow performances is shown in Fig. 4-10 to Fig. 4-12, and the flow rate fluctuation coefficients are listed as Table 4-6. The detailed data of the instantaneous flow rates of curve-sided type helical claw rotors designed in this thesis are listed in Appendix C.

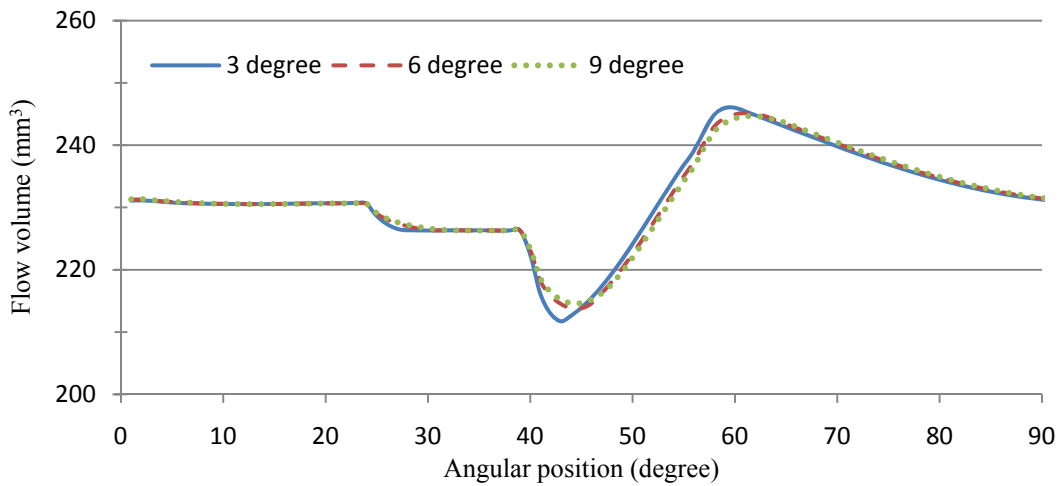


Figure 4-10 Flow rate of 4-claw arc shape curve-sided type pump



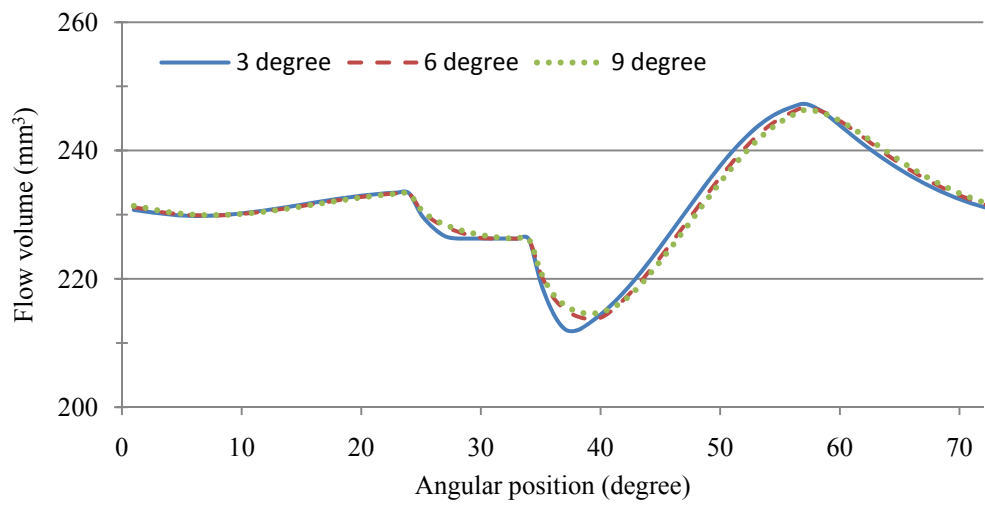


Figure 4-11 Flow rate of 5-claw arc shape curve-sided type pump

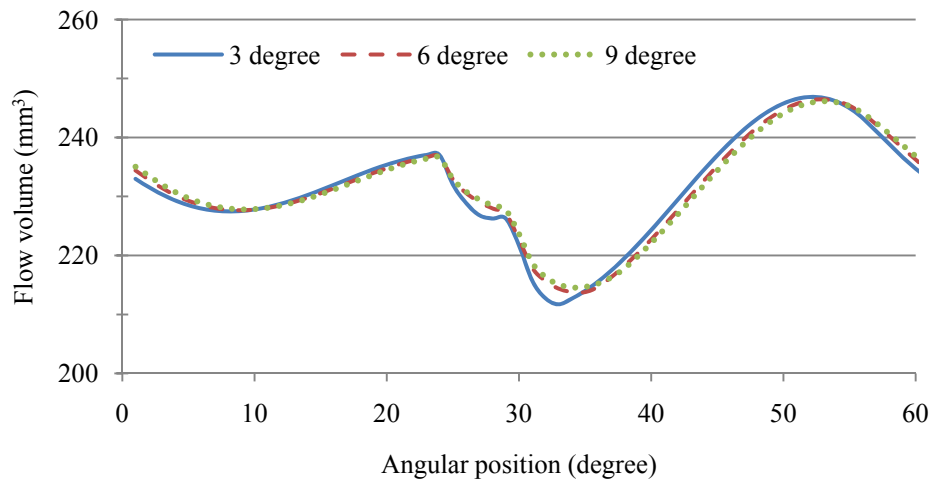


Figure 4-12 Flow rate of 6-claw arc shape curve-sided type pump

Table 4-6 Fluctuation coefficients of arc shape curve-sided type pumps

No. of claws	Helix angle	$\lambda$
4	3°	0.1483
	6°	0.1355
	9°	0.1297
5	3°	0.1529
	6°	0.1425
	9°	0.1372
6	3°	0.1520
	6°	0.1412
	9°	0.1365

The analysis shows that as the helix angle increases, the fluctuation coefficient of the curve-sided type helical claw rotor pump would decrease, and the fluctuation coefficient is lower than the helical claw rotor pump while the helix angle is less than 6°. In the other hand, the discharge flow of the curve-sided type helical claw rotor pump with less claw numbers is smoother than ones with more claw numbers. As Fig. 4-10 shows, the fluctuation of a 4-claw curve-sided type helical claw rotor pump only occurs in less than half period. However, the waveform of the instantaneous flow rate of the

curve-sided type helical claw rotor pump is very similar to the helical claw rotor pump.

The comparison of the instantaneous flow rate between a 4-claw helical claw rotor pump and a 4-claw curve-sided type helical claw rotor pump both with  $6^\circ$  helix angle is shown as Fig. 4-13.

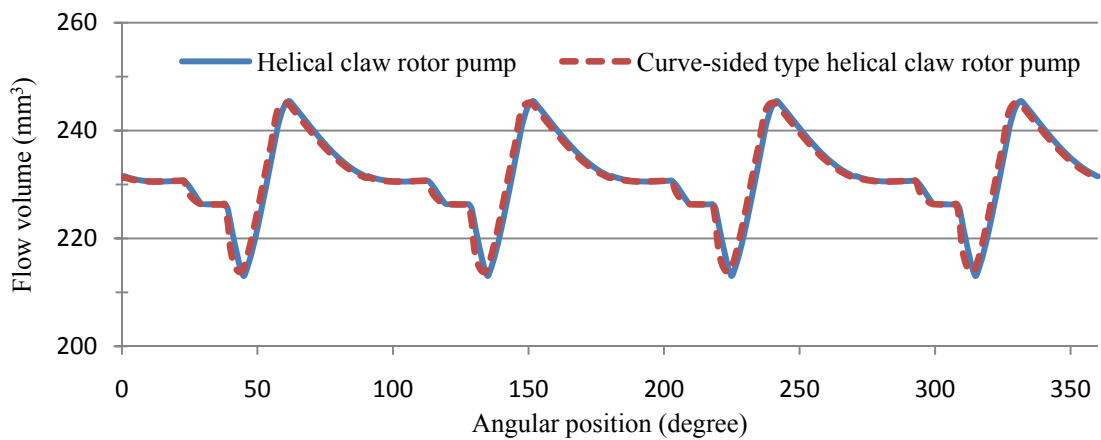


Figure 4-13 Comparison of flow rate between helical and arc shape curve-sided claw rotor pump

The curve shape of the curve-sided type helical claw rotor pair can be adjusted from the arc to the parabola or yoke shape, and the flow conditions of these two different curve-sided type helical claw rotor pumps are also analyzed. The relations between angular position and instantaneous flow rate of the parabolic curve-sided type helical claw rotor pumps of different helix angles and different numbers of claws are shown as Fig. 4-13 to Fig. 4-15, and the fluctuation coefficients are listed as Table 4-7.

The detailed data of the instantaneous flow rates of the parabolic curve-sided type helical claw rotors designed in this thesis are listed in Appendix C.

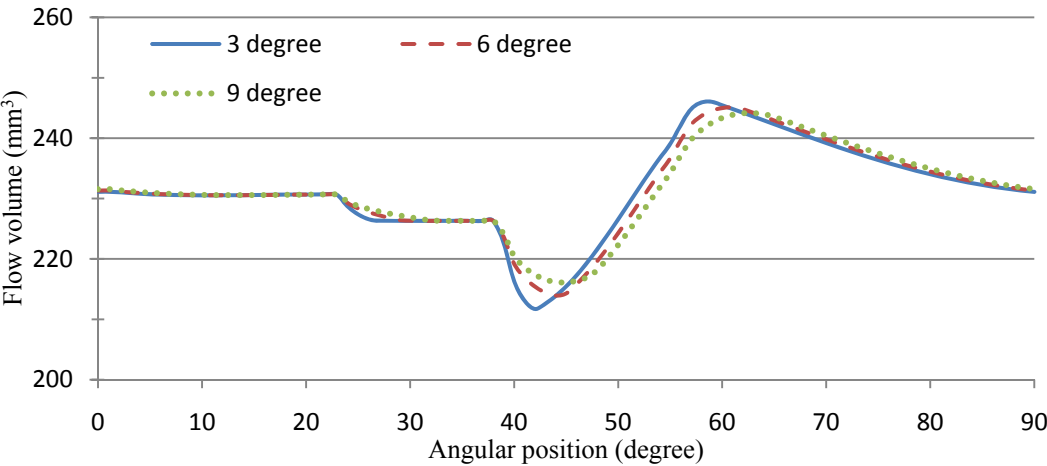


Figure 4-14 Flow rate of 4-claw parabolic curve-sided type pump

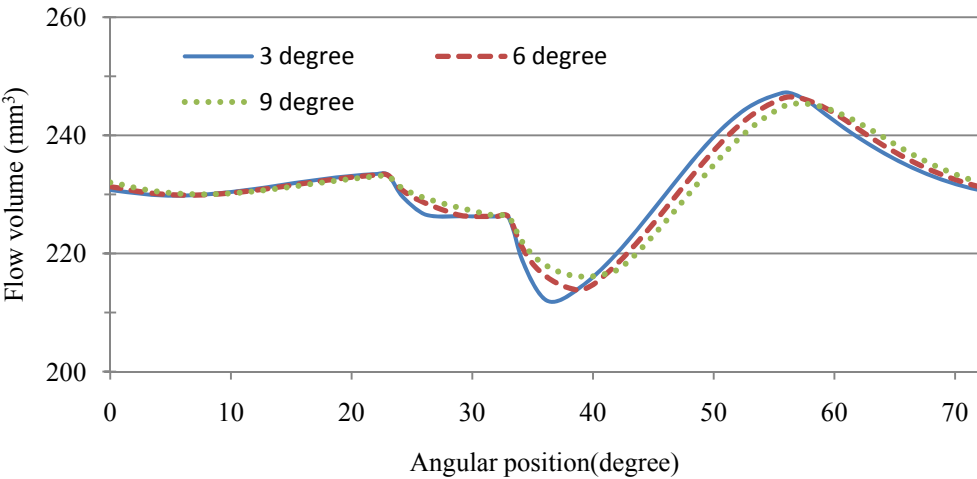


Figure 4-15 Flow rate of 5-claw parabolic curve-sided type pump

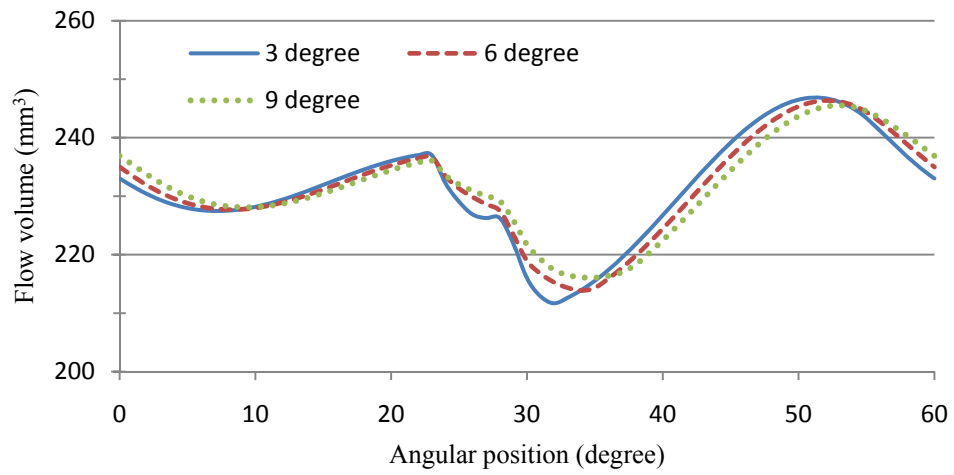


Figure 4-16 Flow rate of 6-claw parabolic curve-sided type pump

Table 4-7 Fluctuation coefficients of parabolic curve-sided type pumps

No. of claws	Helix angle	$\lambda$
4	3°	0.1484
	6°	0.1348
	9°	0.1212
5	3°	0.1529
	6°	0.1411
	9°	0.1268
6	3°	0.1520
	6°	0.1404
	9°	0.1273

The yoke shape curve-sided type helical claw rotor pump is also analyzed. The relations between angular position and instantaneous flow rate of different helix angles and different numbers of claws are shown as Fig. 4-16 to Fig. 4-18, and the fluctuation coefficients are listed as Table 4-8. The detailed data of the instantaneous flow rates of the yoke shape curve-sided type helical claw rotors designed in this thesis are listed in Appendix C.

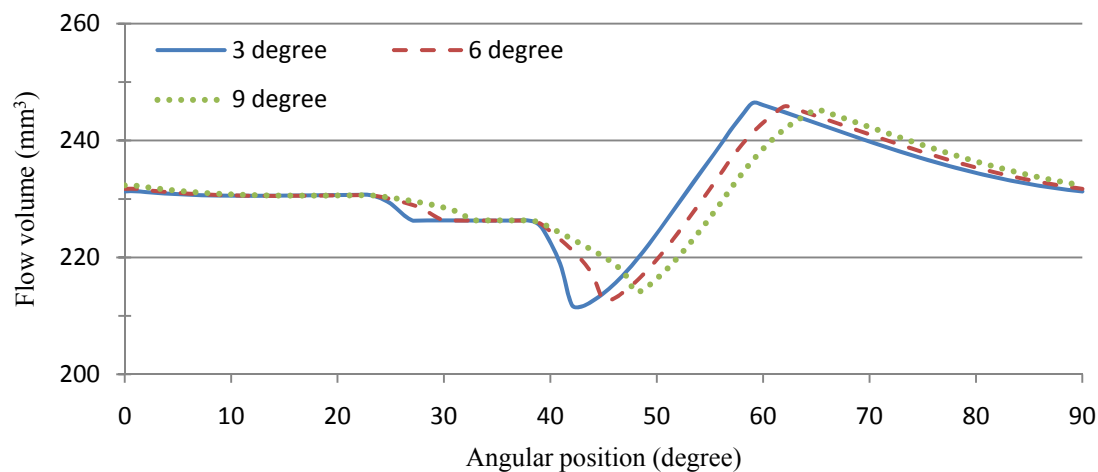


Figure 4-17 Flow rate of 4-claw yoke shape curve-sided type pump

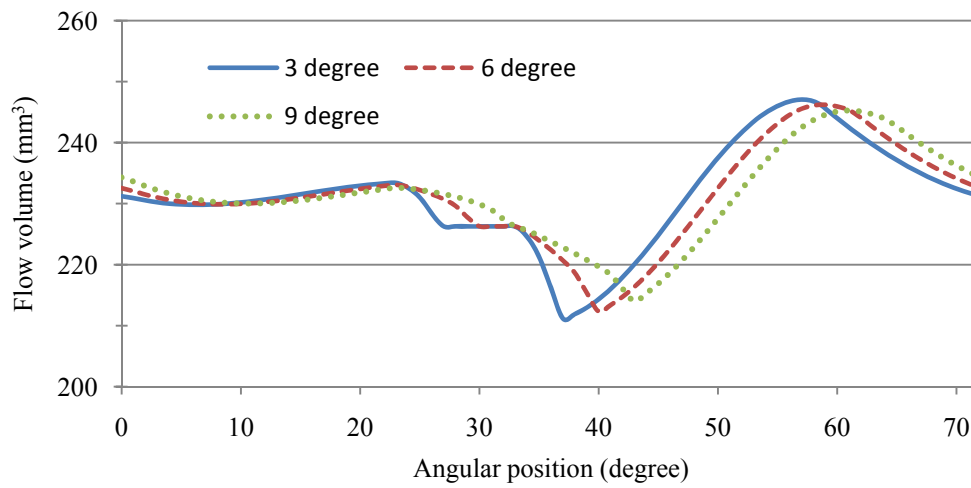


Figure 4-18 Flow rate of 5-claw yoke shape curve-sided type pump

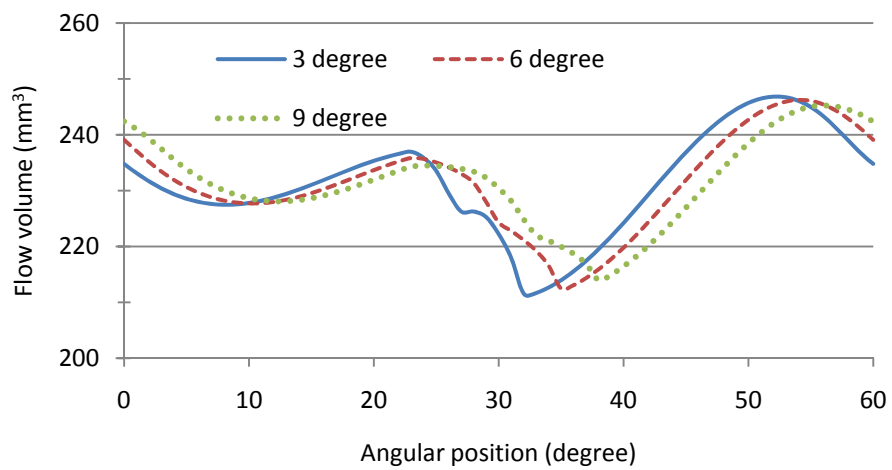


Figure 4-19 Flow rate of 6-claw yoke shape curve-sided type pump

Table 4-8 Fluctuation coefficients of yoke shape curve-sided type pumps

No. of claws	Helix angle	$\lambda$
4	3°	0.1484
	6°	0.1433
	9°	0.1344
5	3°	0.1550
	6°	0.1464
	9°	0.1351
6	3°	0.1524
	6°	0.1460
	9°	0.1351

The results show that the fluctuation coefficients of the arc shape and parabolic curve-sided type helical claw rotor pump are close, and the coefficient of the parabolic is higher than the arc shape while the helix angle is small, but as the growth of helix angle, the coefficient would be lower than the arc shape. In the other hand, the fluctuation coefficient of the yoke shape curve-sided type helical claw rotor pump is higher than the arc and parabolic curve-sided type helical claw rotor pumps, and the discharge flow is not as smooth as the other two types either.



## 4.5 Comparison of the helical designed claw rotor pumps

The discharge flow of the helical claw rotor pump is smoother than the flow of the curve-sided claw rotor pump, but the parabolic curve-sided claw rotor pump has lower fluctuation coefficient because of the relatively low peak value. Since the helix angle of the arc shape curve-sided claw rotor pump is limited, the parabolic and yoke shape curve-sided type helical claw rotor pumps are therefore chosen to compare with the helical claw rotor pump. The comparison chart of the flow rates of different types of 4-claw helical claw rotor pumps all with  $15^\circ$  helix angle are shown as Fig. 4-19, and the fluctuation coefficients are listed as Table 4-9. The result shows that the helical claw rotor pump and parabolic curve-sided type helical claw rotor pump have the similar discharge process which the waveform and fluctuation coefficient are both alike, and can both reduce the flow pulsation.

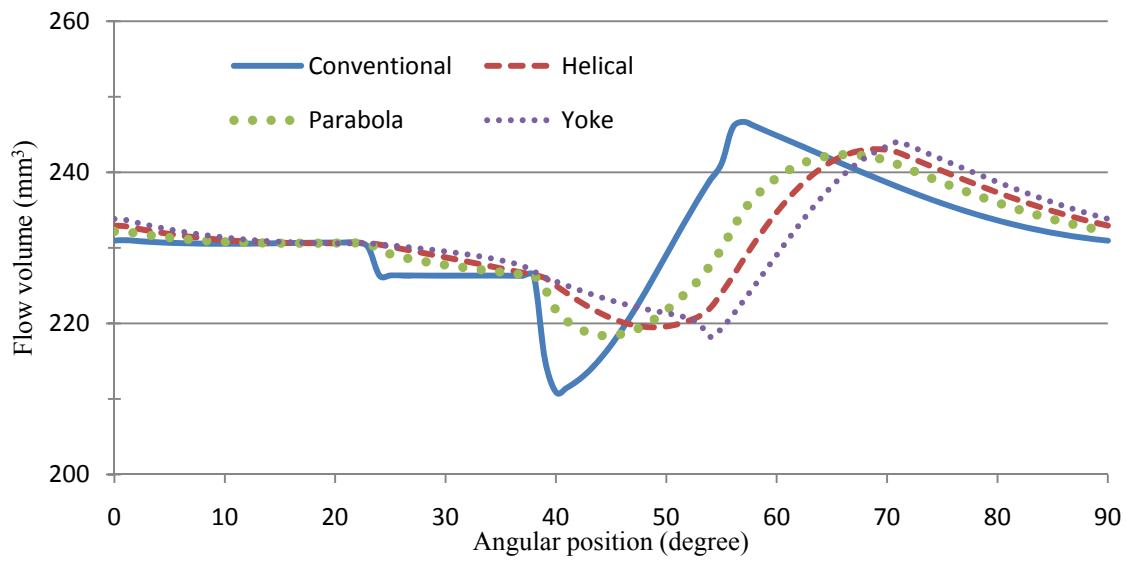


Figure 4-20 Flow rate of different helical types of 4-claw rotor pumps

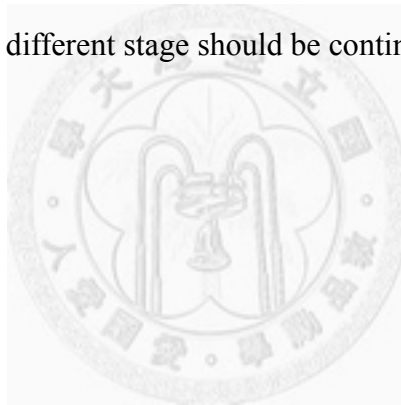
Table 4-9 Fluctuation coefficients of different helical types of claw rotor pumps

No. of claws	Helix angle	Pump type	$\lambda$
4	0°	Conventional	0.1547
		Helical	0.1019
	15°	Parabolic	0.1036
		Yoke shape	0.1116

Since the cross-section areas of the claw rotor pair, the helical claw rotor pair and the curve-sided type helical claw rotor pair are the same, they have the same specific flow rate and area efficiency as well; but due to the longer leakage flow route, the helical claw rotor pump and the curve-sided type helical claw rotor pump would have

lower leakage flow. As equation (2.7), the discharge flow increases as the decrease in the leakage flow, in other words the helical designed claw rotor pumps would have higher volumetric efficiency than the conventional claw rotor pump.

In the other hand, the discharge flow becomes more continuous in the helical and curve-sided type helical claw rotor pump, which reveals that the pulsation problem caused by the periodical fluctuation flow is reduced. The steady output can lead to a longer life time, and it also makes the multi-stage design of claw rotor pump become easier, since the flow rate in different stage should be continuous.



## Chapter 5 Conclusions and suggestions

The claw rotor pump has been expected for its characteristic of high pressure head and good volumetric efficiency. Since there are helical lobe and helical gear pump in order to improve the performances of the traditional lobe and gear pump, helical design can also be the key factor of the claw rotor pump's development. This thesis proves the practicability of the helical design to the claw rotor pump, and the conclusions and suggestions would be described in this chapter.

### 5.1 Conclusions

1. The parametric model of the claw rotor pair's contour is created so every point on the contour can be obtained by inputting the design variables and the angular position, and the cross-section and carry-over area of the claw rotor pair can be obtained as well. A computer program is developed to simulate the discharge flow volume in any designate angular position, so the efficiency and performance of a claw rotor pump can be therefore predicted.
2. The conventional claw rotor pump is examined by the computer program developed in this thesis. The simulation shows that the discharge flow of the claw rotor pump is not continuous and will cause pulsation problem during the operation

process. The simulation also shows that the fluctuation exists no matter what number of claws of the designed claw rotor pair is.

3. Helical claw rotor pairs with different helix angles are designed and analyzed by the computer program developed in this study. The analysis shows that helical design can effectively reduce the fluctuation by making the discharge flow more continuous, and the drop of fluctuation is proportional to the helix angle. In addition, the more the number of claws is, the less the helix angle is needed to completely eliminate the flow fluctuation.
4. The curve-sided type helical rotor pair is designed to make the discharge flow export to two opposite directions, and therefore decrease the stress and bending torque that exert to the pump. The analysis of the performances shows that the curve-sided helical design can reduce the flow fluctuation and provide a smooth discharge.
5. A patent of this innovative helical design of claw rotor is proposed. What is claimed is
  - a. A helical claw rotor pair comprising a pair of conjugate claw rotors' contour and a helical design method.
  - b. A curve-sided type helical claw rotor pair comprising a pair of conjugate claw

rotors' contour and the phase shifting method to make the curve shape.

## 5.2 Suggestions

The performances of the helical claw rotor pump and the curve-sided type helical claw rotor pump are predicted to be better than the conventional claw rotor pump but still require experiments to prove, and further researches are also needed to improve the designs. The further ideas for the study of helical claw rotor pump are suggested as below:

1. The claw tips become sharper because of the helical design, and that would weaken the strength of the rotor pair. In order to avoid fracture, the contour of claw rotor pair is supposed to be modified. The ideal design is making smooth claw tips or larger tip angle to strengthen the claws of claw rotors.
2. The housing chambers and the buffer designs of the helical claw rotor pump and the curve-sided type helical claw rotor pump are needed to be proposed.
3. Since the discharge flow in the new designed helical claw rotor pump is more continuous than the conventional claw rotor pump, the helical claw rotor could apply to the multi-stage design such as series connection. In a series connected claw rotor pump, the export flow of the first stage would be the inlet flow of the

second stage, so the relation between instantaneous flow rate and rotation angle of rotors has to be clarified.



## References

- [1] Richard Dearne, “The Fine Art of Gear Pump Selection and Operation,” World Pumps, pp. 38-40, June, 2001.
- [2] Hydraulics & Pneumatics, “Hydraulic Pump,” Fluid Power Handbook & Directory, pp. 119-127, 1998-1999.
- [3] J S Fleming, Y Tang, G Cook, “The twin helical screw compressor, Part 1: development, applications and competitive position,” Proceedings Institution of Mechanical Engineers, Vol. 212, p.356, 1998.
- [4] Germany patent DE196 29 174 A1, “Claw pump for producing vacuum,” 1998.
- [5] China patent CN2503232Y, “耐高壓多級爪式真空泵,” 2001.
- [6] W. K. Fan, *Design and Analysis of a Claw Rotor Vacuum Pump*, National Taiwan University Master Thesis, pp. 7, July, 2008.
- [7] China patent CN1512064A, “一種用於無油真空泵的漸開線、直線爪型轉子結構,” 2002.
- [8] Chiu-Fan Hsieh, Yii-Wen Hwang, Zhang-Hua Fong, “Study on the tooth profile for the screw claw-type pump,” MECHANISM AND MACHINE THEORY, Vol.43, 812-818, 2008.



- [9] U.S. patent 6,364,642, "ROTARY PISTON MACHINE WITH THREE BLADE ROTORS," 2002
- [10] U.S. patent 7,128,543, "COMPRESSOR MACHINE WITH TWO COUNTER-ROTATING ROTORS," 2006.
- [11] Great Britain patent GB1304394A, "IMPROVEMENTS IN OR RELATING TO ROTARY PISTON COMPRESSORS," 1973.
- [12] C. G. Fu, *Design of a Liquid Pump with New Claw Rotors*, National Taiwan University Master Thesis, pp.96, July, 2009. (Traditional Chinese)
- [13] H. Vogelsang, B. Verhulsdonk, M. Turk, G. Hornig, "Pulsation problems in rotary lobe pumps," World Pumps, Feb., 1999.
- [14] HugoVogelsang Maschinenbau GmbH, <http://www.vogelsang-gmbh.com/>
- [15] Z. H. Zhou, J. H. Yan, L. H. Liu, "Calculation and Analysis of Gap Leakage," *China Academic Journal Electronic Publishing House*, Vol. 4, 2002. (Simplified Chinese)
- [16] L. F. Li, *Improvement of The Volumetric Efficiency and The Machining Tolerance of The Gear Pumps*, National Taiwan University Master Thesis, pp. 39-40, June, 1990. (Traditional Chinese)
- [17] D. Manring, "Measuring Pump Efficiency: Uncertainty Considerations," *ASME*,

Vol. 127, pp. 280~284, Dec, 2005.

[18] Wilson, E. Warren, *Positive-Displacement Pumps and Fluid Motors*, Pitman Publishing Corporation, 1950.

[19] T. S. Lin, *A Study of The Optimum Clearances for External Spur Gear Pumps*, National Tsing Hua University Master Thesis, p. 4, Jun., 2004. (Traditional Chinese)

[20] 黃光裕, “設計合乎齒輪機械定律之齒型與接觸線,” *機械設計原理(下)講義*.

[21] 蔣君宏, *機構學*, pp.306-309, 1955.

[22] K. J. Huang, C. C. Chen, Y. Y. Chang, “Geometric displacement optimization of external helical gear pumps,” *Proceedings of the Institution of Mechanical Engineers*, Sep., 2009

## Appendix A

### AutoLISP program for flow rate calculation

In AutoCAD, the Lisp language is used for parametric model design. Type in “VLISP” in AutoCAD command line, as shown in Fig.A-1, and then the Visual LISP program would be generated. The calculation program developed in this thesis can be therefore edited in the Visual LISP program.

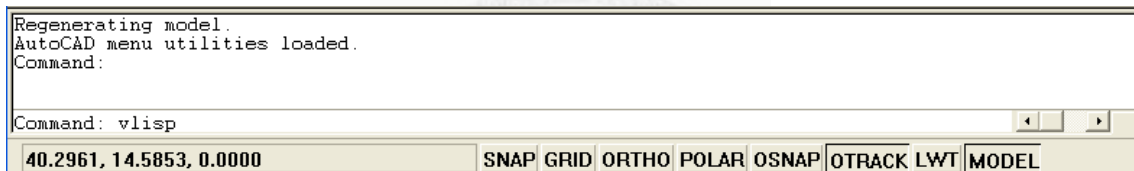


Figure A-1 AutoCAD Text Window

The flow rate calculation program and notes are shown below:

```

; calculation.lsp
(defun c:flow ( / dtheta thetal thet theta phi x1 y1 s1 a1 x2 y2 2rp x2l s2
               thetta2 a2 a3 liquid1 volumel liquid2 volume flowrate flowvolume)
  ;calculation program for conventional claw rotor pump
  (setq r      (getreal "\nInput rotor radius: ")      ;input rotor radius
        rp     (getreal "\nInput pitch radius: ")     ;input pitch radius
        d      (getreal "\nInput rotor depth: ")      ;input rotor depth
        thick  (getreal "\nInput rotor thickness: ")  ;input rotor thickness
        N      (getint "\nInput claw number: ")       ;input claw number
        Q      (getint "\nIteration: ")               ;input iteration number
  )
  (setq dtheta (/ (/ (* 2.0 pi) N) Q)                ;period angle devided by iteration
        thetal (acos (/ rp r))                       ;starting angular position
        thet   (+ thetal (/ (* 2.0 pi) N))           ;ending angular position
        theta  (rotorangle N r rp d thet)            ;real contact angle of the rotor pair
        phi 0.0                                       ;starting rotation angle
        flowvolume 0.0                               ;total flow volume
  )
  (repeat Q      ;starting integration
    (setq rotor1 (areal N r rp d theta 100) ;left rotor area in angular position theta
          rotor2 (area2 N r rp d theta 100) ;right rotor area in angular position theta
    )
    (if (> theta (/ (* 2.0 pi) N))
      (progn
        (setq thetta (- theta (/ (* 2.0 pi) N)))
      )
      (progn
        (setq thetta theta)
      )
    )
    (setq x1 (rotor1x N r rp d thetta) ;x-coordinate value in angular position thetta
          y1 (rotor1y N r rp d thetta) ;y-coordinate value in angular position thetta
          s1 (sqrt (+ (* x1 x1) (* y1 y1))) ;distance of left rotor edge
          a1 (* 0.5 s1 r (sin (- (+ theta phi) (/ (* 2.0 pi) N)))) ;chamber volume 1
          x2 (rotor2x N r rp d thetta)
          y2 (rotor2y N r rp d thetta)
          2rp (* 2.0 rp)
          x2l (- 2rp x2)
          s2 (sqrt (+ (* x2l x2l) (* y2 y2))) ;distance of right rotor edge
    )
    (if (> theta (/ (* 2.0 pi) N))
      (prong
        (setq thetta2 (+ (/ (* 2.0 pi) N) (atan (/ y2 x2l))) )
      )
      (prong
        (setq thetta2 (atan (/ y2 x2l)) )
      )
    )
    (setq a2 (* 0.5 s2 r (sin (- (+ thetta2 phi) (/ (* 2.0 pi) N)))) ;chamber volume 2
          a3 (* r r (- (/ (* 2.0 pi) N) phi)) ;chamber volume 3
    )
    (setq liquid1 (- (+ a1 a2 a3) (+ rotor1 rotor2)) ;liquid area of position1
          volumel (* liquid1 thick) ;liquid volume of postion1
    )
  )

```

```

(setq phi (+ phi dtheta)
  thet (- thet dtheta)
  theta (rotorangle N r rp d thet)
)

(setq rotor1 (areal N r rp d theta 100)
  rotor2 (area2 N r rp d theta 100)
)

(if (> theta (/ (* 2.0 pi) N))
  (progn
    (setq thetta (- theta (/ (* 2.0 pi) N)))
  )
  (progn
    (setq thetta theta)
  )
)
)
(setq x1 (rotor1x N r rp d thetta)
  y1 (rotor1y N r rp d thetta)
  s1 (sqrt (+ (* x1 x1) (* y1 y1)))
  a1 (* 0.5 s1 r (sin (- (+ theta phi) (/ (* 2.0 pi) N))))
  x2 (rotor2x N r rp d thetta)
  y2 (rotor2y N r rp d thetta)
  2rp (* 2.0 rp)
  x2l (- 2rp x2)
  s2 (sqrt (+ (* x2l x2l) (* y2 y2)))
)
(if (> theta (/ (* 2.0 pi) N))
  (progn
    (setq thetta2 (+ (/ (* 2.0 pi) N) (atan (/ y2 x2l))) )
  )
  (progn
    (setq thetta2 (atan (/ y2 x2l)) )
  )
)
)
(setq a2 (* 0.5 s2 r (sin (- (+ thetta2 phi) (/ (* 2.0 pi) N)))) )
(setq a3 (* r r (- (/ (* 2.0 pi) N) phi)) )
(setq liquid2 (- (+ a1 a2 a3) (+ rotor1 rotor2)) ;liquid area of position2 )
(setq volume2 (* liquid2 thick) ) ;liquid volume of position2
(setq flowrate (- volumel volume2) ) ;flow between position 1&2
(setq flowvolume (+ flowvolume flowrate) ) ;total discharge
(princ "rotation angle: ") (princ (rtd phi))(princ " ")
(princ "flow:")(princ flowrate)(princ "\n")

);ed repeat

(princ "flow per claw: ")(princ flowvolume)(princ)

) ; end_defun flow

=====

(defun c:helixflow ( / dtheta thetal thet theta phi flowvolume volumel volume2
  flowrate) ;calculation program for the helical claw rotor pump
(setq r (getreal "\nInput rotor radius: ")

```

```

rp  (getreal "\nInput pitch radius: ")
d   (getreal "\nInput rotor depth: ")
syi (getreal "\nInput helix angle: ")           ;helix angle
thick (getreal "\nInput rotor thickness: ")
N    (getint  "\nInput claw number: ")
Q    (getint  "\nIteration: ")
)
(setq dtheta (/ (/ (* 2.0 pi) N) Q)
thetal (acos (/ rp r))
thet (+ thetal (/ (* 2.0 pi) N))
theta (rotorangle N r rp d thet)
phi 0.0
syi (dtr syi) ;rotation angle in radian
flowvolume 0.0
)
(repeat Q
  (setq volumel (helicalvolume N r rp d thet phi syi thick) )
  ;liquid volume in angular position1
  (setq phi (+ phi dtheta)
    thet (- thet dtheta)
  )
  (setq volume2 (helicalvolume N r rp d thet phi syi thick) )
  ;liquid volume in angular position2

  (setq flowrate (- volumel volume2)
    flowvolume (+ flowvolume flowrate)
  )

  (princ "rotation angle: ") (princ (rtd phi))(princ " ")
  (princ "flow: ")(princ flowrate)(princ "\n")
);end repeat
(princ "flow per claw: ")(princ flowvolume)(princ
) ; end_defun helixflow

;=====

(defun c:curveflow ( / dtheta thetal thet theta phi flowvolume flowrate volumel volume2 )
;calculation program for the curve-sided type helical claw rotor pump
(setq r  (getreal "\nInput rotor radius: ")
rp  (getreal "\nInput pitch radius: ")
d   (getreal "\nInput rotor depth: ")
syi (getreal "\nInput helical angle: ")
thick (getreal "\nInput rotor thickness: ")
N    (getint  "\nInput claw number: ")
Q    (getint  "\nIteration: ")
)
(setq dtheta (/ (/ (* 2.0 pi) N) Q)
thetal (acos (/ rp r))
thet (+ thetal (/ (* 2.0 pi) N))
theta (rotorangle N r rp d thet)
phi 0.0
syi (dtr syi)
flowvolume 0.0
)

```

```

(repeat Q
  (setq volume1 (* 2.0 (curvevolume N r rp d thet phi syi thick)) )
  ;liquid volume in angular position1

  (setq phi (+ phi dtheta)
    thet (- thet dtheta)
  )
  (setq volume2 (* 2.0 (curvevolume N r rp d thet phi syi thick))
    ;liquid volume in angular position2
  )
  (setq flowrate (- volume1 volume2)
    flowvolume (+ flowvolume flowrate)
  )

  (princ "rotation angle: ") (princ (rtd phi))(princ " ")
  (princ "flow: ")(princ flowrate)(princ "\n")
);end repeat

(princ "flow per claw: ")(princ flowvolume)(princ)

) ; end_defun curveflow

```

The AutoLISP file of the calculation program is saved in the AutoCAD working directory, and can be loaded by typing in “(load “calculation.lsp”)” in the command line, as shown in Fig. A-2.



Figure A-2 Loading the calculation program

The flow rate calculation program includes 5 types of claw rotor pump, and the relationships between commands and pump types are listed in Table A-1. For example, type in “FLOW” in the command line to analyze the instantaneous flow rate of the

conventional claw rotor pump, and then the flow volume in every angular position would be listed in the AutoCAD text window, as shown in Fig. A-3 and A-4.

Table A-1 AutoLISP commands to analyze different type of claw rotor pump

Command	Pump type
FLOW	Conventional claw rotor pump
HELIXFLOW	Helical claw rotor pump
CURVEFLOW	Arc shape curve-sided type helical claw rotor pump
PARABOLAFLOW	Parabolic curve-sided type helical claw rotor pump
YOKEFLOW	Yoke shape curve-sided type helical claw rotor pump

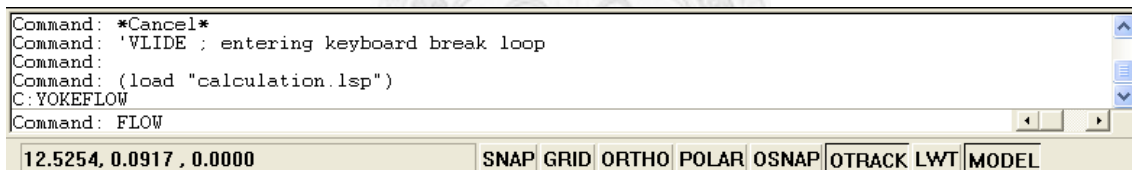


Figure A-3 Flow rate calculation commands (FLOW)



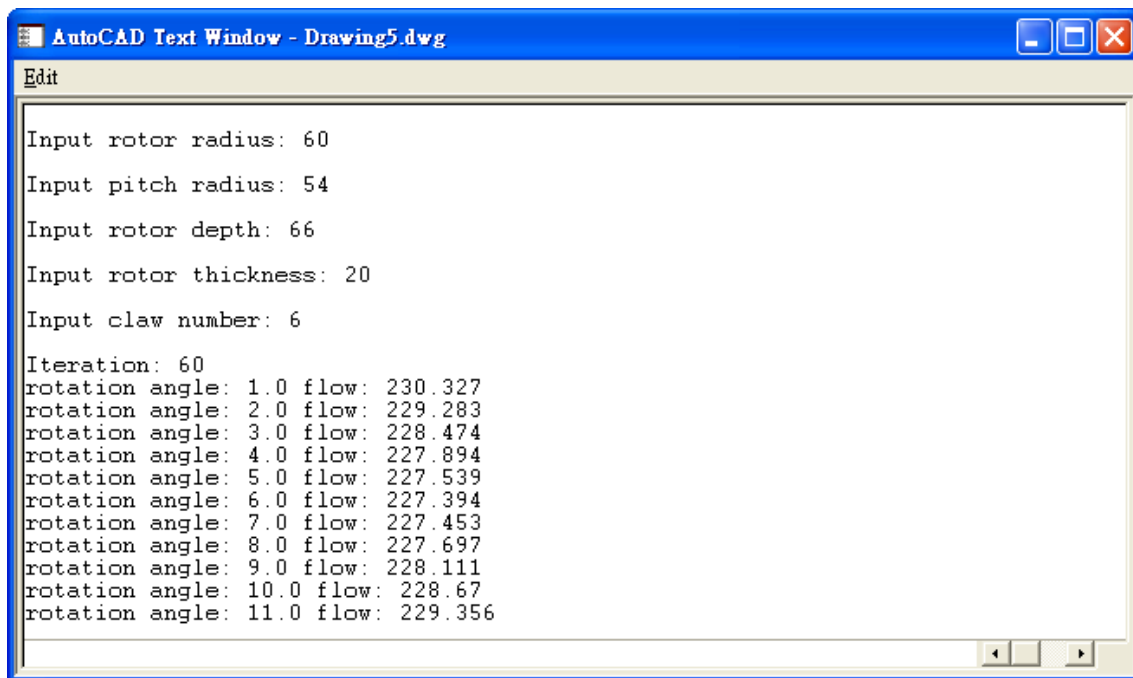
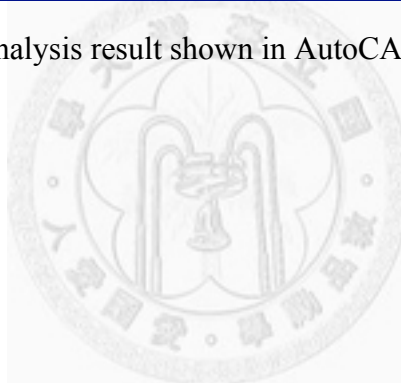


Figure A-4 Analysis result shown in AutoCAD text window



## Appendix B Flow rate data of claw rotor pump

The tables listed below are the detailed data of the flow volume per rotation angle ( $\text{mm}^3/\text{degree}$ ) of different designate helix angles for the helical claw rotor pumps (i.e. conventional claw rotor pumps when helix angle =  $0^\circ$ ). The horizontal axis represents the helix angle and the vertical axis represents the angular position. The table of contents represents the discharge flow volume during one rotation angle.

Table B-1 Data of 4-claw helical claw rotor pump

	$0^\circ$	$3^\circ$	$6^\circ$	$9^\circ$	$12^\circ$	$18^\circ$	$24^\circ$	$30^\circ$
$0^\circ$	230.944	231.197	231.52	231.915	232.385	233.537	234.937	236.516
$1^\circ$	231.015	231.247	231.539	231.902	232.338	233.426	234.772	236.313
$2^\circ$	230.908	231.097	231.353	231.681	232.08	233.097	234.381	235.874
$3^\circ$	230.801	230.968	231.193	231.484	231.847	232.792	234.011	235.453
$4^\circ$	230.725	230.856	231.05	231.309	231.637	232.51	233.662	235.05
$5^\circ$	230.654	230.768	230.931	231.156	231.449	232.251	233.335	234.666
$6^\circ$	230.61	230.691	230.828	231.023	231.283	232.014	233.03	234.301
$7^\circ$	230.569	230.637	230.746	230.91	231.138	231.8	232.746	233.955
$8^\circ$	230.552	230.591	230.679	230.816	231.013	231.607	232.484	233.63
$9^\circ$	230.535	230.564	230.627	230.739	230.907	231.435	232.243	233.324
$10^\circ$	230.536	230.544	230.59	230.677	230.817	231.283	232.023	233.039
$11^\circ$	230.534	230.538	230.564	230.631	230.746	231.15	231.823	232.773
$12^\circ$	230.557	230.537	230.551	230.597	230.688	231.036	231.643	232.527
$13^\circ$	230.559	230.546	230.545	230.575	230.644	230.938	231.482	232.3
$14^\circ$	230.589	230.559	230.549	230.563	230.613	230.856	231.338	232.091
$15^\circ$	230.603	230.576	230.557	230.559	230.591	230.788	231.212	231.901
$16^\circ$	230.627	230.596	230.571	230.562	230.58	230.734	231.102	231.728
$17^\circ$	230.654	230.616	230.588	230.571	230.576	230.692	231.007	231.572
$18^\circ$	230.663	230.638	230.607	230.584	230.579	230.66	230.927	231.432

19°	230.686	230.658	230.627	230.601	230.586	230.638	230.859	231.308
20°	230.701	230.676	230.646	230.617	230.598	230.624	230.802	231.197
21°	230.705	230.691	230.665	230.636	230.611	230.616	230.757	231.1
22°	230.715	230.703	230.681	230.653	230.626	230.614	230.72	231.016
23°	230.028	230.689	230.681	230.658	230.632	230.609	230.685	230.936
24°	226.332	229.732	230.201	230.34	230.393	230.438	230.529	230.763
25°	226.333	228.273	229.477	229.864	230.042	230.203	230.332	230.563
26°	226.334	226.833	228.75	229.385	229.687	229.967	230.138	230.372
27°	226.326	226.331	228.021	228.904	229.332	229.734	229.95	230.192
28°	226.322	226.329	227.29	228.42	228.975	229.499	229.766	230.015
29°	226.321	226.326	226.57	227.935	228.614	229.266	229.585	229.846
30°	226.321	226.323	226.327	227.448	228.253	229.031	229.406	229.684
31°	226.319	226.32	226.324	226.959	227.89	228.795	229.228	229.525
32°	226.311	226.317	226.321	226.48	227.524	228.559	229.05	229.37
33°	226.309	226.315	226.319	226.323	227.159	228.32	228.874	229.221
34°	226.307	226.312	226.316	226.32	226.792	228.082	228.698	229.072
35°	226.305	226.309	226.313	226.317	226.433	227.839	228.522	228.925
36°	226.303	226.307	226.311	226.315	226.319	227.599	228.346	228.783
37°	226.3	226.304	226.308	226.312	226.316	227.355	228.169	228.639
38°	226.297	226.301	226.305	226.309	226.313	227.111	227.989	228.497
39°	215.137	224.916	225.583	225.808	225.923	226.589	227.588	228.163
40°	210.878	219.919	223.072	224.127	224.654	225.49	226.764	227.508
41°	211.485	214.872	220.55	222.444	223.394	224.42	225.955	226.868
42°	212.435	211.471	218.159	220.851	222.202	223.55	225.181	226.245
43°	213.706	212.056	215.955	219.384	221.099	222.822	224.454	225.672
44°	215.281	213.167	213.993	218.077	220.121	222.169	223.786	225.146
45°	217.13	214.59	213.036	216.962	219.288	221.615	223.191	224.668
46°	219.215	216.297	214.198	216.067	218.616	221.173	222.674	224.267
47°	221.493	218.257	215.737	215.417	218.131	220.849	222.261	223.938
48°	223.933	220.432	217.54	215.528	217.845	220.665	222.075	223.677
49°	226.473	222.782	219.572	217.097	217.763	220.61	222.041	223.512
50°	229.077	225.261	221.794	218.954	217.9	220.709	222.115	223.43
51°	231.685	227.823	224.164	221.013	218.643	220.944	222.298	223.425
52°	234.251	230.415	226.636	223.233	220.476	221.33	222.584	223.518
53°	236.716	232.989	229.163	225.574	222.513	221.851	222.979	223.699
54°	239.036	235.489	231.694	227.988	224.683	222.507	223.473	224.053

55°	241.147	237.866	234.177	230.428	226.943	223.286	224.06	224.528
56°	245.915	240.463	236.768	232.986	229.358	224.249	224.79	225.12
57°	246.672	243.422	239.493	235.654	231.902	225.673	225.648	225.795
58°	246.082	245.498	241.712	237.992	234.24	227.632	226.477	226.466
59°	245.478	246.314	243.41	239.976	236.346	229.55	227.285	227.116
60°	244.863	245.768	244.609	241.603	238.204	231.389	228.069	227.731
61°	244.24	245.159	245.336	242.874	239.801	233.129	228.827	228.342
62°	243.61	244.54	245.421	243.795	241.131	234.756	229.56	228.93
63°	242.977	243.914	244.832	244.381	242.191	236.248	230.489	229.483
64°	242.342	243.283	244.212	244.65	242.981	237.597	231.807	230.03
65°	241.708	242.65	243.586	244.487	243.51	238.786	233.087	230.556
66°	241.078	242.016	242.956	243.881	243.788	239.81	234.306	231.045
67°	240.453	241.385	242.325	243.257	243.828	240.659	235.452	231.53
68°	239.835	240.758	241.694	242.63	243.542	241.33	236.511	231.993
69°	239.227	240.137	241.067	242.004	242.931	241.822	237.472	232.615
70°	238.63	239.524	240.445	241.379	242.31	242.136	238.324	233.551
71°	238.046	238.922	239.831	240.758	241.69	242.28	239.059	234.452
72°	237.476	238.332	239.226	240.143	241.072	242.257	239.671	235.304
73°	236.923	237.756	238.631	239.537	240.46	242.084	240.155	236.1
74°	236.388	237.196	238.05	238.941	239.854	241.689	240.51	236.83
75°	235.873	236.653	237.484	238.357	239.258	241.092	240.735	237.482
76°	235.377	236.128	236.934	237.786	238.672	240.495	240.83	238.051
77°	234.903	235.623	236.401	237.23	238.099	239.904	240.8	238.532
78°	234.452	235.139	235.888	236.692	237.54	239.322	240.652	238.915
79°	234.024	234.677	235.395	236.172	236.997	238.75	240.394	239.202
80°	233.62	234.237	234.923	235.671	236.471	238.189	239.976	239.39
81°	233.241	233.822	234.474	235.19	235.964	237.643	239.414	239.475
82°	232.886	233.431	234.047	234.732	235.476	237.111	238.86	239.463
83°	232.557	233.064	233.645	234.295	235.01	236.595	238.317	239.358
84°	232.253	232.723	233.267	233.882	234.564	236.097	237.787	239.161
85°	231.974	232.406	232.913	233.493	234.142	235.618	237.27	238.882
86°	231.72	232.115	232.585	233.128	233.742	235.159	236.769	238.477
87°	231.49	231.849	232.282	232.788	233.367	234.721	236.284	237.967
88°	231.285	231.608	232.003	232.473	233.015	234.304	235.816	237.469
89°	231.103	231.391	231.749	232.182	232.688	233.909	235.367	236.985
90°	230.944	231.197	231.52	231.915	232.385	233.537	234.937	236.516

Table B-2 Data of 5-claw helical claw rotor pump

	0°	3°	6°	9°	12°	18°	24°	30°
0°	230.342	230.98	231.889	233.073	234.527	238.022	239.315	237.507
1°	230.199	230.709	231.483	232.531	233.852	237.248	239.127	237.903
2°	229.984	230.366	231.006	231.918	233.102	236.261	238.66	238.017
3°	229.846	230.109	230.619	231.395	232.443	235.341	238.109	238.037
4°	229.784	229.932	230.316	230.96	231.873	234.506	237.488	237.967
5°	229.794	229.834	230.097	230.611	231.389	233.757	236.815	237.813
6°	229.861	229.804	229.955	230.344	230.992	233.093	236.109	237.577
7°	229.992	229.844	229.887	230.157	230.677	232.514	235.385	237.268
8°	230.166	229.941	229.888	230.045	230.441	232.017	234.647	236.895
9°	230.388	230.093	229.95	230.002	230.281	231.602	233.975	236.465
10°	230.641	230.289	230.069	230.023	230.191	231.264	233.382	235.991
11°	230.921	230.526	230.236	230.103	230.167	231	232.865	235.488
12°	231.221	230.791	230.445	230.234	230.202	230.807	232.422	234.965
13°	231.527	231.079	230.688	230.41	230.291	230.68	232.051	234.434
14°	231.841	231.38	230.957	230.623	230.427	230.615	231.748	233.899
15°	232.142	231.688	231.244	230.865	230.603	230.605	231.51	233.421
16°	232.433	231.994	231.541	231.129	230.811	230.646	231.333	233.007
17°	232.707	232.289	231.839	231.407	231.045	230.73	231.211	232.655
18°	232.945	232.567	232.132	231.691	231.296	230.852	231.141	232.361
19°	233.156	232.822	232.412	231.973	231.558	231.006	231.117	232.122
20°	233.329	233.046	232.671	232.247	231.822	231.183	231.134	231.932
21°	233.459	233.235	232.904	232.504	232.082	231.378	231.185	231.789
22°	233.541	233.384	233.106	232.74	232.33	231.584	231.266	231.688
23°	232.426	233.454	233.249	232.931	232.547	231.783	231.359	231.613
24°	226.29	231.915	232.558	232.553	232.333	231.699	231.258	231.398
25°	226.289	229.509	231.43	231.885	231.908	231.499	231.091	231.152
26°	226.283	227.118	230.268	231.184	231.455	231.284	230.931	230.932
27°	226.281	226.285	229.082	230.456	230.979	231.064	230.781	230.739
28°	226.279	226.283	227.878	229.702	230.477	230.826	230.635	230.561
29°	226.278	226.281	226.684	228.927	229.95	230.576	230.489	230.402
30°	226.275	226.279	226.282	228.136	229.403	230.308	230.342	230.259
31°	226.273	226.276	226.28	227.332	228.838	230.022	230.189	230.123
32°	226.271	226.274	226.277	226.538	228.254	229.721	230.028	229.997
33°	225.418	226.259	226.267	226.27	227.652	229.392	229.852	229.87

34°	210.639	223.298	224.747	225.234	226.257	228.507	229.242	229.389
35°	211.014	218.141	222.17	223.515	224.374	227.292	228.411	228.762
36°	211.74	213.184	219.686	221.859	222.946	226.109	227.593	228.149
37°	212.803	211.474	217.351	220.305	221.783	224.949	226.801	227.561
38°	214.182	212.369	215.225	218.887	220.722	223.863	226.044	227.018
39°	215.856	213.59	213.363	217.642	219.788	222.843	225.34	226.515
40°	217.789	215.113	213.312	216.6	219.009	221.928	224.705	226.063
41°	219.944	216.911	214.663	215.786	218.401	221.132	224.144	225.679
42°	222.286	218.95	216.296	215.232	217.98	220.741	223.667	225.356
43°	224.763	221.19	218.182	215.973	217.764	220.601	223.283	225.102
44°	227.334	223.59	220.284	217.678	217.758	220.598	222.991	224.929
45°	229.945	226.104	222.562	219.609	217.975	220.746	222.803	224.828
46°	232.545	228.682	224.973	221.728	219.197	221.029	222.723	224.801
47°	235.083	231.275	227.47	223.995	221.127	221.466	222.759	224.859
48°	237.506	233.83	230.005	226.367	223.215	222.031	223.11	224.985
49°	239.759	236.295	232.526	228.796	225.421	222.733	223.638	225.178
50°	241.795	238.617	234.982	231.234	227.702	223.548	224.251	225.443
51°	243.563	240.747	237.322	233.631	230.011	224.479	224.941	225.761
52°	245.016	242.633	239.495	235.937	232.302	226.041	225.701	226.124
53°	246.111	244.227	241.45	238.102	234.525	227.978	226.512	226.547
54°	246.805	245.485	243.139	240.076	236.633	229.93	227.359	227.163
55°	247.473	246.387	244.529	241.821	238.584	231.861	228.229	227.856
56°	247.294	247.072	245.663	243.346	240.372	233.753	229.118	228.573
57°	245.616	247.045	246.27	244.452	241.835	235.483	229.956	229.233
58°	244.006	246.29	246.336	245.117	242.944	237.022	231.154	229.84
59°	242.469	244.804	245.929	245.37	243.707	238.357	232.495	230.404
60°	241.009	243.233	245.125	245.246	244.14	239.485	233.751	230.908
61°	239.629	241.737	243.994	244.786	244.261	240.398	234.908	231.367
62°	238.332	240.318	242.539	244.039	244.092	241.098	235.957	231.79
63°	237.121	238.982	241.086	243.055	243.662	241.583	236.889	232.17
64°	235.998	237.73	239.713	241.88	243.002	241.859	237.697	232.866
65°	234.966	236.565	238.423	240.522	242.148	241.933	238.374	233.683
66°	234.027	235.49	237.218	239.196	241.14	241.815	238.915	234.445
67°	233.18	234.506	236.102	237.955	240.012	241.519	239.319	235.147
68°	232.428	233.614	235.075	236.799	238.77	241.061	239.583	235.782
69°	231.768	232.816	234.14	235.732	237.578	240.459	239.711	236.339

70°	231.202	232.111	233.297	234.754	236.473	239.735	239.704	236.815
71°	230.727	231.5	232.546	233.868	235.455	238.915	239.57	237.207
72°	230.342	230.98	231.889	233.073	234.527	238.022	239.315	237.507

Table B-3 Data of 6-claw helical claw rotor pump

	0°	3°	6°	9°	12°	18°	24°	30°
0°	231.49	233.912	236.996	239.857	241.561	241.371	239.86	237.779
1°	230.327	232.401	235.161	238.21	240.387	241.218	240.118	238.337
2°	229.283	231.007	233.424	236.409	238.943	240.734	240.055	238.601
3°	228.474	229.848	231.918	234.661	237.414	240.078	239.826	238.722
4°	227.894	228.924	230.645	233.056	235.859	239.277	239.446	238.708
5°	227.539	228.232	229.605	231.671	234.338	238.358	238.933	238.568
6°	227.394	227.765	228.796	230.516	232.914	237.352	238.305	238.31
7°	227.453	227.516	228.213	229.589	231.652	236.292	237.584	237.947
8°	227.697	227.473	227.849	228.886	230.608	235.21	236.791	237.494
9°	228.111	227.623	227.693	228.401	229.784	234.142	235.952	236.964
10°	228.67	227.95	227.735	228.125	229.175	233.123	235.091	236.375
11°	229.356	228.433	227.958	228.046	228.772	232.188	234.235	235.743
12°	230.14	229.051	228.344	228.152	228.567	231.373	233.41	235.087
13°	230.997	229.781	228.874	228.426	228.545	230.715	232.643	234.427
14°	231.897	230.595	229.525	228.848	228.693	230.242	231.96	233.78
15°	232.81	231.467	230.271	229.399	228.993	229.948	231.388	233.168
16°	233.711	232.367	231.087	230.053	229.425	229.819	230.955	232.61
17°	234.568	233.267	231.944	230.788	229.969	229.841	230.681	232.127
18°	235.354	234.138	232.815	231.576	230.6	229.998	230.554	231.736
19°	236.046	234.952	233.672	232.391	231.295	230.272	230.561	231.46
20°	236.622	235.684	234.487	233.206	232.028	230.645	230.686	231.312
21°	237.062	236.311	235.235	233.995	232.775	231.095	230.91	231.281
22°	237.354	236.813	235.891	234.732	233.511	231.603	231.216	231.349
23°	235.711	237.118	236.403	235.368	234.188	232.128	231.569	231.485
24°	226.263	234.866	235.566	235.083	234.181	232.237	231.593	231.362
25°	226.261	231.212	233.988	234.301	233.819	232.176	231.506	231.174
26°	226.259	227.542	232.303	233.42	233.38	232.098	231.441	231.028

27°	226.257	226.26	230.536	232.448	232.869	232.009	231.382	230.924
28°	226.255	226.258	228.708	231.394	232.282	231.886	231.327	230.848
29°	213.869	224.559	225.996	229.663	231.145	231.394	230.966	230.521
30°	210.865	219.472	222.828	226.779	229.137	230.341	230.15	229.827
31°	211.5	214.441	220.312	223.885	227.089	229.256	229.33	229.154
32°	212.476	211.377	217.935	221.083	225.057	228.181	228.521	228.505
33°	213.776	212.086	215.748	219.231	223.085	227.105	227.728	227.895
34°	215.374	213.223	213.804	217.937	221.201	226.077	226.971	227.321
35°	217.242	214.67	213.033	216.839	219.468	225.083	226.255	226.797
36°	219.344	216.399	214.263	215.963	218.53	224.167	225.59	226.328
37°	221.64	218.378	215.826	215.332	218.057	223.327	224.987	225.917
38°	224.087	220.569	217.649	215.574	217.786	222.587	224.457	225.564
39°	226.638	222.932	219.698	217.191	217.725	221.962	224.01	225.282
40°	229.244	225.42	221.934	219.066	217.876	221.452	223.649	225.066
41°	231.852	227.987	224.315	221.14	218.72	221.107	223.383	224.925
42°	234.412	230.581	226.794	223.373	220.588	221.32	223.215	224.86
43°	236.87	233.151	229.324	225.722	222.638	221.858	223.155	224.868
44°	239.174	235.646	231.854	228.14	224.818	222.521	223.21	224.945
45°	241.272	238.011	234.333	230.581	227.084	223.31	223.744	225.096
46°	243.116	240.197	236.709	232.994	229.391	224.206	224.508	225.309
47°	244.657	242.152	238.931	235.33	231.691	225.53	225.358	225.604
48°	245.85	243.828	240.948	237.537	233.937	227.452	226.272	226.281
49°	246.654	245.179	242.712	239.567	236.08	229.404	227.232	227.12
50°	247.031	246.162	244.176	241.37	238.072	231.341	228.508	227.982
51°	246.945	246.736	245.296	242.9	239.865	233.219	230.236	228.848
52°	246.367	246.867	246.031	244.112	241.412	234.994	231.923	229.693
53°	245.271	246.521	246.343	244.965	242.67	236.622	233.527	230.775
54°	243.664	245.672	246.199	245.42	243.596	238.061	235.007	232.174
55°	241.364	244.289	245.565	245.439	244.149	239.265	236.322	233.468
56°	238.94	242.373	244.426	244.999	244.3	240.201	237.436	234.625
57°	236.735	240.141	242.881	244.153	244.077	240.87	238.346	235.637
58°	234.755	237.86	241.045	242.965	243.517	241.279	239.05	236.502
59°	233.006	235.772	239.042	241.508	242.663	241.442	239.553	237.216
60°	231.49	233.912	236.996	239.857	241.561	241.371	239.86	237.779



## Appendix C Flow rate data of curve-sided type helical claw rotor pumps

### C.1 Flow rate data of the arc shape type

The tables listed below are the detailed data of the flow volume per rotation angle ( $\text{mm}^3/\text{degree}$ ) of different designate helix angles for the arc shape curve-sided type helical claw rotor pumps. The horizontal axis represents the helix angle and the vertical axis represents the angular position. The table of contents represents the discharge flow volume during one rotation angle.

Table C-1 Data of 4-claw arc shape curve-sided type helical claw rotor pump

	3°	6°	9°
0°	231.1	231.248	231.325
1°	231.159	231.293	231.363
2°	231.023	231.139	231.203
3°	230.904	231.006	231.062
4°	230.804	230.891	230.94
5°	230.725	230.797	230.84
6°	230.658	230.718	230.754
7°	230.611	230.659	230.689
8°	230.574	230.611	230.636
9°	230.553	230.579	230.599
10°	230.539	230.557	230.572
11°	230.537	230.547	230.557
12°	230.542	230.546	230.553
13°	230.551	230.549	230.553
14°	230.569	230.563	230.563

15°	230.585	230.575	230.574
16°	230.608	230.595	230.592
17°	230.629	230.615	230.61
18°	230.649	230.634	230.628
19°	230.669	230.655	230.649
20°	230.685	230.671	230.665
21°	230.698	230.686	230.68
22°	230.709	230.699	230.693
23°	230.596	230.611	230.611
24°	228.603	229.029	229.11
25°	227.358	228.07	228.208
26°	226.546	227.456	227.639
27°	226.329	226.999	227.218
28°	226.327	226.64	226.901
29°	226.325	226.378	226.663
30°	226.322	226.324	226.48
31°	226.319	226.321	226.359
32°	226.315	226.317	226.318
33°	226.313	226.315	226.316
34°	226.31	226.312	226.313
35°	226.308	226.31	226.311
36°	226.305	226.307	226.308
37°	226.303	226.304	226.305
38°	226.3	226.302	226.303
39°	222.408	223.191	223.345
40°	216.058	218.199	218.621
41°	212.955	215.863	216.444
42°	211.725	214.505	215.196
43°	212.632	213.864	214.653
44°	213.919	213.817	214.677
45°	215.503	214.632	215.225
46°	217.356	216.272	216.26
47°	219.439	218.163	217.744
48°	221.718	220.274	219.766
49°	224.145	222.56	221.973
50°	226.676	224.981	224.325

51°	229.262	227.488	226.777
52°	231.85	230.033	229.279
53°	234.39	232.565	231.783
54°	236.829	235.032	234.239
55°	239.114	237.383	236.593
56°	242.265	240.422	239.609
57°	244.941	243.045	242.229
58°	245.951	244.31	243.561
59°	246.022	244.951	244.304
60°	245.432	245.163	244.636
61°	244.817	245.059	244.665
62°	244.194	244.628	244.465
63°	243.565	244.006	244.088
64°	242.933	243.378	243.57
65°	242.299	242.747	242.942
66°	241.666	242.115	242.312
67°	241.037	241.485	241.683
68°	240.413	240.859	241.057
69°	239.796	240.239	240.437
70°	239.189	239.627	239.823
71°	238.594	239.025	239.22
72°	238.011	238.435	238.627
73°	237.444	237.858	238.047
74°	236.893	237.297	237.482
75°	236.359	236.752	236.933
76°	235.845	236.225	236.402
77°	235.352	235.718	235.889
78°	234.88	235.232	235.397
79°	234.43	234.768	234.927
80°	234.004	234.326	234.478
81°	233.602	233.907	234.053
82°	233.225	233.513	233.651
83°	232.872	233.143	233.274
84°	232.544	232.797	232.921
85°	232.242	232.477	232.594
86°	231.965	232.182	232.291

87°	231.712	231.912	232.013
88°	231.485	231.666	231.759
89°	231.281	231.445	231.53
90°	231.1	231.248	231.325

Table C-2 Data of 5-claw arc shape curve-sided type helical claw rotor pump

	3°	6°	9°
0°	230.732	231.14	231.367
1°	230.509	230.853	231.051
2°	230.213	230.494	230.664
3°	230.002	230.222	230.363
4°	229.867	230.028	230.142
5°	229.81	229.914	230.001
6°	229.818	229.869	229.931
7°	229.892	229.894	229.932
8°	230.019	229.976	229.991
9°	230.198	230.115	230.109
10°	230.416	230.297	230.272
11°	230.67	230.521	230.479
12°	230.948	230.775	230.718
13°	231.245	231.052	230.983
14°	231.552	231.345	231.266
15°	231.858	231.644	231.558
16°	232.16	231.943	231.852
17°	232.447	232.234	232.141
18°	232.712	232.508	232.415
19°	232.951	232.761	232.67
20°	233.156	232.985	232.899
21°	233.323	233.175	233.096
22°	233.448	233.326	233.256
23°	233.333	233.277	233.225
24°	230.051	230.706	230.799
25°	227.99	229.143	229.342
26°	226.64	228.14	228.424
27°	226.284	227.393	227.746
28°	226.282	226.801	227.229

29°	226.28	226.367	226.838
30°	226.277	226.279	226.538
31°	226.275	226.277	226.339
32°	226.273	226.274	226.275
33°	226.182	226.2	226.204
34°	219.421	220.815	221.089
35°	214.792	217.224	217.709
36°	212.173	215.28	215.893
37°	211.928	214.177	214.918
38°	213.007	213.754	214.563
39°	214.399	213.925	214.77
40°	216.079	215.133	215.495
41°	218.015	216.862	216.672
42°	220.171	218.834	218.384
43°	222.505	221.009	220.473
44°	224.975	223.348	222.736
45°	227.53	225.804	225.127
46°	230.123	228.33	227.603
47°	232.702	230.877	230.112
48°	235.213	233.393	232.606
49°	237.606	235.827	235.033
50°	239.828	238.128	237.342
51°	241.829	240.243	239.483
52°	243.559	242.125	241.406
53°	244.972	243.724	243.062
54°	246.025	244.995	244.407
55°	246.775	245.976	245.471
56°	247.29	246.706	246.29
57°	246.653	246.447	246.161
58°	245.465	245.688	245.546
59°	243.925	244.628	244.633
60°	242.395	243.379	243.525
61°	240.941	242.022	242.3
62°	239.568	240.607	241.018
63°	238.277	239.26	239.723
64°	237.073	237.998	238.446

65°	235.958	236.821	237.245
66°	234.933	235.734	236.131
67°	234	234.737	235.107
68°	233.16	233.832	234.174
69°	232.414	233.02	233.334
70°	231.761	232.301	232.586
71°	231.201	231.675	231.931
72°	230.732	231.14	231.367

Table C-3 Data of 6-claw arc shape curve-sided type helical claw rotor pump

	3°	6°	9°
0°	232.981	234.396	235.038
1°	231.599	232.853	233.496
2°	230.335	231.425	232.019
3°	229.308	230.231	230.754
4°	228.512	229.269	229.72
5°	227.946	228.538	228.915
6°	227.601	228.03	228.335
7°	227.468	227.74	227.972
8°	227.534	227.655	227.818
9°	227.784	227.763	227.858
10°	228.2	228.048	228.078
11°	228.762	228.49	228.46
12°	229.445	229.068	228.983
13°	230.225	229.76	229.625
14°	231.075	230.538	230.36
15°	231.966	231.377	231.164
16°	232.869	232.248	232.007
17°	233.757	233.123	232.863
18°	234.599	233.974	233.703
19°	235.371	234.774	234.501
20°	236.047	235.497	235.232
21°	236.607	236.121	235.871
22°	237.032	236.626	236.399
23°	237.008	236.751	236.567

24°	232.025	232.916	232.974
25°	228.878	230.586	230.827
26°	226.807	229.086	229.477
27°	226.259	227.957	228.472
28°	226.257	227.055	227.699
29°	221.716	222.763	223.663
30°	215.708	217.921	218.756
31°	212.722	215.675	216.361
32°	211.708	214.386	215.096
33°	212.676	213.792	214.578
34°	213.989	213.795	214.67
35°	215.596	214.706	215.246
36°	217.468	216.368	216.299
37°	219.57	218.279	217.853
38°	221.862	220.405	219.891
39°	224.301	222.705	222.112
40°	226.839	225.135	224.474
41°	229.427	227.648	226.933
42°	232.015	230.195	229.438
43°	234.55	232.725	231.941
44°	236.979	235.186	234.392
45°	239.251	237.527	236.737
46°	241.315	239.696	238.928
47°	243.122	241.644	240.913
48°	244.623	243.322	242.644
49°	245.775	244.685	244.075
50°	246.537	245.688	245.163
51°	246.87	246.293	245.866
52°	246.74	246.462	246.147
53°	246.117	246.163	245.972
54°	244.984	245.373	245.318
55°	243.277	244.035	244.127
56°	241.117	242.24	242.484
57°	238.852	240.257	240.642
58°	236.675	238.226	238.731
59°	234.713	236.247	236.84

60°	232.981	234.396	235.038
-----	---------	---------	---------

## C.2 Flow rate data of the parabolic type

The tables listed below are the detailed data of the flow volume per rotation angle ( $\text{mm}^3/\text{degree}$ ) of different designate helix angles for the parabolic curve-sided type helical claw rotor pumps. The horizontal axis represents the helix angle and the vertical axis represents the angular position. The table of contents represents the discharge flow volume during one rotation angle.

Table C-4 Data of 4-claw parabolic curve-sided type helical claw rotor pump

	3°	6°	9°
0°	231.107	231.31	231.555
1°	231.165	231.349	231.573
2°	231.029	231.189	231.389
3°	230.909	231.049	231.227
4°	230.808	230.927	231.084
5°	230.728	230.828	230.964
6°	230.66	230.744	230.861
7°	230.613	230.679	230.776
8°	230.575	230.627	230.708
9°	230.554	230.591	230.655
10°	230.539	230.565	230.615
11°	230.537	230.551	230.588
12°	230.542	230.547	230.571
13°	230.551	230.548	230.563
14°	230.569	230.56	230.564
15°	230.584	230.571	230.569



16°	230.608	230.59	230.581
17°	230.628	230.609	230.596
18°	230.648	230.628	230.612
19°	230.669	230.649	230.63
20°	230.684	230.665	230.647
21°	230.697	230.681	230.663
22°	230.708	230.695	230.677
23°	230.6	230.621	230.62
24°	228.676	229.254	229.501
25°	227.427	228.375	228.785
26°	226.57	227.757	228.286
27°	226.329	227.249	227.876
28°	226.327	226.808	227.514
29°	226.325	226.425	227.191
30°	226.322	226.325	226.896
31°	226.319	226.321	226.621
32°	226.315	226.318	226.375
33°	226.313	226.316	226.319
34°	226.311	226.313	226.316
35°	226.308	226.311	226.313
36°	226.305	226.308	226.311
37°	226.303	226.305	226.308
38°	226.3	226.303	226.305
39°	222.558	223.623	224.098
40°	216.337	219.21	220.484
41°	213.108	216.929	218.621
42°	211.71	215.408	217.387
43°	212.593	214.43	216.584
44°	213.867	213.92	216.171
45°	215.44	214.281	216.108
46°	217.282	215.816	216.374
47°	219.357	217.627	216.959
48°	221.628	219.666	218.17
49°	224.05	221.894	220.147
50°	226.577	224.267	222.302
51°	229.161	226.742	224.596

52°	231.749	229.268	226.983
53°	234.291	231.797	229.416
54°	236.734	234.276	231.846
55°	239.026	236.655	234.224
56°	242.144	239.618	237.106
57°	244.827	242.238	239.713
58°	245.913	243.687	241.368
59°	246.042	244.556	242.541
60°	245.455	245	243.354
61°	244.841	245.103	243.863
62°	244.218	244.809	244.118
63°	243.59	244.192	244.142
64°	242.957	243.565	243.97
65°	242.323	242.936	243.537
66°	241.691	242.305	242.911
67°	241.061	241.675	242.285
68°	240.437	241.048	241.659
69°	239.82	240.426	241.036
70°	239.213	239.812	240.419
71°	238.617	239.207	239.809
72°	238.034	238.614	239.208
73°	237.466	238.033	238.619
74°	236.914	237.467	238.042
75°	236.38	236.918	237.48
76°	235.865	236.386	236.934
77°	235.371	235.873	236.405
78°	234.898	235.381	235.896
79°	234.448	234.91	235.406
80°	234.021	234.461	234.938
81°	233.618	234.036	234.492
82°	233.239	233.634	234.069
83°	232.886	233.257	233.669
84°	232.557	232.904	233.293
85°	232.254	232.577	232.942
86°	231.975	232.274	232.615
87°	231.722	231.996	232.314

88°	231.493	231.743	232.036
89°	231.288	231.515	231.784
90°	231.107	231.31	231.555

Table C-5 Data of 5-claw parabolic curve-sided type helical claw rotor pump

	3°	6°	9°
0°	230.749	231.313	232.035
1°	230.523	230.999	231.633
2°	230.224	230.613	231.159
3°	230.01	230.315	230.773
4°	229.872	230.097	230.469
5°	229.812	229.959	230.249
6°	229.817	229.892	230.102
7°	229.889	229.895	230.03
8°	230.013	229.959	230.023
9°	230.191	230.08	230.078
10°	230.407	230.248	230.186
11°	230.66	230.458	230.343
12°	230.937	230.702	230.54
13°	231.234	230.971	230.769
14°	231.54	231.258	231.024
15°	231.846	231.554	231.295
16°	232.148	231.852	231.577
17°	232.435	232.145	231.86
18°	232.701	232.422	232.136
19°	232.941	232.681	232.401
20°	233.148	232.913	232.646
21°	233.317	233.112	232.864
22°	233.444	233.275	233.053
23°	233.338	233.261	233.092
24°	230.172	231.057	231.332
25°	228.104	229.637	230.215
26°	226.68	228.635	229.441
27°	226.284	227.808	228.801
28°	226.282	227.08	228.226
29°	226.28	226.445	227.706

30°	226.277	226.28	227.225
31°	226.275	226.277	226.773
32°	226.273	226.275	226.368
33°	226.186	226.21	226.223
34°	219.667	221.559	222.397
35°	215.041	218.284	219.726
36°	212.261	216.309	218.113
37°	211.898	214.991	217.029
38°	212.963	214.174	216.372
39°	214.343	213.828	216.092
40°	216.012	214.735	216.125
41°	217.938	216.378	216.51
42°	220.086	218.272	217.217
43°	222.413	220.38	218.794
44°	224.878	222.664	220.837
45°	227.43	225.077	223.046
46°	230.022	227.576	225.377
47°	232.601	230.109	227.785
48°	235.116	232.628	230.224
49°	237.513	235.079	232.643
50°	239.742	237.412	234.992
51°	241.752	239.576	237.222
52°	243.493	241.521	239.282
53°	244.919	243.199	241.124
54°	245.986	244.562	242.701
55°	246.747	245.637	244.024
56°	247.272	246.456	245.108
57°	246.677	246.377	245.422
58°	245.523	245.804	245.284
59°	243.987	244.9	244.822
60°	242.454	243.764	244.109
61°	240.997	242.469	243.201
62°	239.621	241.046	242.149
63°	238.327	239.675	240.997
64°	237.12	238.388	239.778
65°	236.001	237.186	238.512

66°	234.972	236.072	237.318
67°	234.036	235.049	236.211
68°	233.193	234.116	235.194
69°	232.443	233.277	234.267
70°	231.786	232.53	233.431
71°	231.222	231.875	232.687
72°	230.749	231.313	232.035

Table C-6 Data of 6-claw parabolic curve-sided type helical claw rotor pump

	3°	6°	9°
0°	233.047	234.991	236.888
1°	231.656	233.383	235.325
2°	230.383	231.885	233.736
3°	229.346	230.621	232.29
4°	228.542	229.589	231.036
5°	227.967	228.788	230.01
6°	227.613	228.212	229.209
7°	227.472	227.856	228.63
8°	227.53	227.707	228.264
9°	227.773	227.755	228.101
10°	228.183	227.984	228.129
11°	228.739	228.376	228.332
12°	229.418	228.91	228.693
13°	230.194	229.564	229.19
14°	231.041	230.313	229.802
15°	231.931	231.13	230.504
16°	232.834	231.987	231.271
17°	233.722	232.857	232.075
18°	234.567	233.711	232.891
19°	235.341	234.523	233.69
20°	236.022	235.266	234.448
21°	236.586	235.917	235.14
22°	237.016	236.455	235.744
23°	237.01	236.654	236.066
24°	232.209	233.408	233.557

25°	229.053	231.317	231.99
26°	226.868	229.834	230.915
27°	226.259	228.59	230.014
28°	226.257	227.483	229.187
29°	221.889	223.386	225.85
30°	215.982	218.946	221.706
31°	212.863	216.745	219.223
32°	211.685	215.265	217.396
33°	212.636	214.327	216.494
34°	213.936	213.856	216.116
35°	215.531	214.333	216.066
36°	217.394	215.905	216.366
37°	219.487	217.736	216.972
38°	221.772	219.793	218.275
39°	224.205	222.034	220.268
40°	226.739	224.418	222.437
41°	229.326	226.9	224.74
42°	231.914	229.429	227.133
43°	234.451	231.957	229.569
44°	236.885	234.431	231.998
45°	239.164	236.801	234.371
46°	241.236	239.015	236.638
47°	243.053	241.022	238.748
48°	244.566	242.775	240.652
49°	245.732	244.226	242.304
50°	246.509	245.332	243.657
51°	246.859	246.051	244.669
52°	246.747	246.346	245.299
53°	246.144	246.183	245.51
54°	245.031	245.539	245.275
55°	243.346	244.357	244.54
56°	241.205	242.713	243.359
57°	238.943	240.837	241.913
58°	236.759	238.86	240.304
59°	234.788	236.883	238.607
60°	233.047	234.991	236.888

### C.3 Flow rate data of the yoke shape type

The tables listed below are the detailed data of the flow volume per rotation angle ( $\text{mm}^3/\text{degree}$ ) of different designate helix angles for the yoke shape curve-sided type helical claw rotor pumps. The horizontal axis represents the helix angle and the vertical axis represents the angular position. The table of contents represents the discharge flow volume during one rotation angle.

Table C-7 Data of 4-claw yoke shape curve-sided type helical claw rotor pump

	3°	6°	9°
0°	231.289	231.746	232.319
1°	231.329	231.745	232.275
2°	231.168	231.534	232.016
3°	231.03	231.354	231.785
4°	230.907	231.189	231.578
5°	230.811	231.049	231.39
6°	230.724	230.93	231.229
7°	230.664	230.827	231.085
8°	230.61	230.746	230.964
9°	230.579	230.677	230.861
10°	230.551	230.629	230.774
11°	230.542	230.588	230.707
12°	230.535	230.566	230.651
13°	230.543	230.549	230.613
14°	230.55	230.547	230.583
15°	230.569	230.547	230.568
16°	230.585	230.559	230.558

17°	230.606	230.57	230.56
18°	230.628	230.589	230.564
19°	230.648	230.606	230.577
20°	230.669	230.627	230.59
21°	230.683	230.647	230.608
22°	230.697	230.664	230.625
23°	230.691	230.668	230.629
24°	230.151	230.401	230.452
25°	229.203	230.003	230.205
26°	227.602	229.55	229.94
27°	226.332	229.02	229.645
28°	226.33	228.348	229.321
29°	226.328	227.217	228.953
30°	226.325	226.33	228.515
31°	226.321	226.327	227.968
32°	226.318	226.325	227.045
33°	226.316	226.322	226.327
34°	226.314	226.318	226.324
35°	226.31	226.316	226.322
36°	226.308	226.313	226.319
37°	226.305	226.311	226.316
38°	226.302	226.308	226.313
39°	225.492	225.853	225.974
40°	222.547	224.473	225.064
41°	218.475	222.983	224.121
42°	211.924	221.327	223.167
43°	211.649	219.429	222.187
44°	212.6	216.88	221.177
45°	213.873	212.697	220.097
46°	215.444	213.02	218.868
47°	217.284	214.27	217.149
48°	219.358	215.81	214.161
49°	221.626	217.611	214.871
50°	224.046	219.64	216.351
51°	226.573	221.859	218.082
52°	229.153	224.223	220.031



53°	231.741	226.689	222.161
54°	234.281	229.208	224.431
55°	236.723	231.729	226.796
56°	239.243	234.331	229.304
57°	241.921	236.962	231.882
58°	244.268	239.311	234.313
59°	246.402	241.348	236.559
60°	246.058	243.069	238.596
61°	245.455	244.544	240.393
62°	244.841	245.855	241.938
63°	244.218	245.425	243.225
64°	243.59	244.813	244.306
65°	242.957	244.193	245.251
66°	242.324	243.567	244.781
67°	241.691	242.938	244.166
68°	241.061	242.307	243.545
69°	240.437	241.677	242.92
70°	239.821	241.05	242.293
71°	239.213	240.429	241.668
72°	238.617	239.815	241.046
73°	238.034	239.21	240.429
74°	237.466	238.617	239.819
75°	236.915	238.036	239.218
76°	236.381	237.471	238.629
77°	235.866	236.921	238.052
78°	235.372	236.389	237.49
79°	234.899	235.877	236.944
80°	234.448	235.384	236.415
81°	234.021	234.913	235.905
82°	233.618	234.465	235.416
83°	233.24	234.039	234.947
84°	232.886	233.637	234.501
85°	232.558	233.26	234.077
86°	232.254	232.907	233.677
87°	231.976	232.579	233.301
88°	231.723	232.277	232.949

89°	231.494	231.999	232.622
90°	231.289	231.746	232.319

Table C-8 Data of 5-claw yoke shape curve-sided type helical claw rotor pump

	3°	6°	9°
0°	231.224	232.54	234.293
1°	230.91	232.046	233.62
2°	230.524	231.48	232.871
3°	230.227	231.007	232.216
4°	230.01	230.62	231.65
5°	229.875	230.319	231.172
6°	229.811	230.101	230.783
7°	229.819	229.96	230.476
8°	229.888	229.894	230.25
9°	230.015	229.894	230.102
10°	230.19	229.958	230.024
11°	230.408	230.076	230.015
12°	230.659	230.244	230.065
13°	230.938	230.452	230.171
14°	231.232	230.695	230.323
15°	231.539	230.963	230.517
16°	231.845	231.25	230.744
17°	232.147	231.545	230.996
18°	232.434	231.843	231.266
19°	232.7	232.134	231.546
20°	232.94	232.413	231.827
21°	233.146	232.671	232.105
22°	233.315	232.902	232.368
23°	233.413	233.08	232.591
24°	232.592	232.782	232.491
25°	231.05	232.228	232.248
26°	228.395	231.552	231.948
27°	226.287	230.724	231.575
28°	226.285	229.633	231.124
29°	226.282	227.758	230.577
30°	226.279	226.284	229.893

31°	226.277	226.282	229.004
32°	226.275	226.28	227.474
33°	226.256	226.26	226.265
34°	224.57	225.37	225.637
35°	221.307	223.95	224.714
36°	216.189	222.411	223.766
37°	211.175	220.684	222.814
38°	211.905	218.647	221.815
39°	212.969	215.389	220.781
40°	214.348	212.337	219.674
41°	216.015	213.383	218.34
42°	217.94	214.735	216.065
43°	220.085	216.368	214.017
44°	222.411	218.252	215.317
45°	224.874	220.352	216.887
46°	227.425	222.625	218.697
47°	230.015	225.031	220.713
48°	232.592	227.521	222.896
49°	235.105	230.047	225.204
50°	237.502	232.558	227.592
51°	239.729	235.004	230.012
52°	241.737	237.332	232.415
53°	243.477	239.491	234.752
54°	244.902	241.433	236.971
55°	245.984	243.117	239.032
56°	246.776	244.537	240.907
57°	247.026	245.534	242.47
58°	246.812	246.085	243.694
59°	245.595	246.201	244.567
60°	243.989	245.911	245.088
61°	242.456	245.314	245.259
62°	241	244.035	245.089
63°	239.623	242.508	244.605
64°	238.33	241.058	243.886
65°	237.122	239.688	242.627
66°	236.004	238.4	241.186

67°	234.975	237.199	239.824
68°	234.039	236.085	238.544
69°	233.195	235.06	237.349
70°	232.445	234.128	236.241
71°	231.788	233.287	235.222
72°	231.224	232.54	234.293

Table C-9 Data of 6-claw yoke shape curve-sided type helical claw rotor pump

	3°	6°	9°
0°	234.795	239.106	242.395
1°	233.17	237.103	241.021
2°	231.662	235.144	239.31
3°	230.39	233.413	237.463
4°	229.352	231.913	235.567
5°	228.548	230.647	233.847
6°	227.972	229.612	232.355
7°	227.618	228.807	231.091
8°	227.476	228.228	230.055
9°	227.533	227.867	229.244
10°	227.776	227.714	228.652
11°	228.184	227.757	228.273
12°	228.739	227.981	228.096
13°	229.417	228.367	228.109
14°	230.192	228.896	228.297
15°	231.038	229.545	228.642
16°	231.927	230.288	229.124
17°	232.83	231.101	229.722
18°	233.717	231.954	230.412
19°	234.561	232.821	231.167
20°	235.335	233.674	231.964
21°	236.015	234.484	232.774
22°	236.58	235.227	233.571
23°	236.966	235.844	234.294
24°	235.858	235.675	234.496
25°	233.569	235.052	234.445

26°	229.507	234.18	234.265
27°	226.261	233.015	233.927
28°	226.259	231.396	233.42
29°	225.274	227.976	232.304
30°	222.234	224.325	230.434
31°	218.006	222.807	228.178
32°	211.571	221.149	224.892
33°	211.665	219.219	222.06
34°	212.643	216.564	221.05
35°	213.941	212.476	219.962
36°	215.535	213.061	218.712
37°	217.396	214.336	216.915
38°	219.487	215.898	214.01
39°	221.77	217.72	214.933
40°	224.201	219.766	216.435
41°	226.734	221.998	218.185
42°	229.319	224.374	220.151
43°	231.905	226.847	222.294
44°	234.441	229.368	224.574
45°	236.873	231.889	226.945
46°	239.151	234.357	229.362
47°	241.222	236.721	231.775
48°	243.037	238.931	234.134
49°	244.55	240.935	236.389
50°	245.715	242.684	238.491
51°	246.491	244.133	240.39
52°	246.84	245.238	242.038
53°	246.728	245.956	243.391
54°	246.126	246.253	244.405
55°	245.003	246.089	245.038
56°	243.351	245.447	245.261
57°	241.287	244.363	245.086
58°	238.962	242.895	244.53
59°	236.766	241.112	243.621
60°	234.795	239.106	242.395

# Vitae

## 作者簡歷

**Name:** Hsin-Wei Wang 王心偉

**Date of birth:** July 31, 1985

**Phone:** +886-916-082812

**E-mail:** [r97522632@ntu.edu.tw](mailto:r97522632@ntu.edu.tw)

### **Educational background:**

- |           |   |
|-----------|---|
| 1991-1994 | Taipei Private Chinshin Elementary School<br>台北市私立靜心小學  |
| 1994-1997 | Taipei Private Tsai Hsing Elementary School<br>台北市私立再興小學  |
| 1997-2000 | Taipei Private Tsai Hsing High School<br>台北市私立再興中學國中部   |
| 2000-2003 | Taipei Private Tsai Hsing High School<br>台北市私立再興中學  |
| 2003-2008 | B.S., Department of Mechanical Engineering, National Taiwan University, Taipei, Taiwan<br>國立台灣大學機械工程學系        |
| 2008-2010 | M.S., Institute of Mechanical Engineering, National Taiwan University, Taipei, Taiwan<br>國立台灣大學機械工程系研究所碩士班設計組 |